ELSEVIER

Chemical Geology 198 (2003) 77–106

CHEMICAL GEOLOGY
INCLUDING
ISOTOPE GEOSCIENCE

www.elsevier.com/locate/chemgeo

# Variation in apatite fission-track length measurement: implications for thermal history modelling

Jocelyn Barbarand[1], Tony Hurford*, Andy Carter

*London Fission-Track Research Group, Research School of Earth Sciences at University College London and Birkbeck College, Gower Street, London WC1E 6BT, UK*

Received 18 April 2002; accepted 6 December 2002

**Abstract**

Predictive thermal history modelling using apatite fission-track (FT) data is dependent on an algorithm to describe the time and temperature dependency of FT annealing which, in turn, relies on the empirical determination of FT length as a measure of the annealing process. Assessment of variation in FT length measurement is poorly described, with few comparisons between analysts and little interlaboratory standardisation. Using apatites of various compositions containing induced tracks annealed to differing degrees, this study has assessed variation in horizontal confined track-length measurement for a variety of procedural conditions.

Replicate analysis by a single observer is typically within 3% but increases inversely with track length. Comparison between observers on the same samples shows significant, generally nonsystematic variation between observers; for a complex length distribution variation is $\sim$ 12%. Sources of variation are identified as: (a) variation from track revelation, including etching, track-in-track (TINT) vs. track-in-cleavage (TINCLE) measurement and use of $^{252}$Cf irradiation to produce additional etching channels; (b) bias in measurement, including equipment, analytical procedures, and sample size; and (c) observer bias, principally differences in and consistency of personal technique.

5 M $HNO_3$ of is preferred to weaker etchants: although more anisotropic, tracks are better defined, permitting more rigorous measurement, while *c*-axis parallel sections (where $2\pi/4\ \pi$ geometry is better defined) are more easily identified. For all but the longest length distributions, TINCLEs are significantly longer than TINTS, with few short TINCLEs at high angles; measurement of TINCLEs effectively masks the anisotropy of annealing. $^{252}$Cf irradiation is effective in increasing the number of TINTs sampled and measured. Variation between values measured for unirradiated and Cf-irradiated aliquots does not exceed that found for a single analyst, although a slight systematic shift to longer lengths for Cf-irradiated samples is seen. As reported by other workers, track-length distributions are anisotropic, anisotropy increasing with annealing level. Track angle exerts a major influence on measured length, summing affects from annealing and etching anisotropies with observer bias. Track angle should be accommodated within the annealing algorithm.

It is recommended that similar track revelation, observation and measurement conditions are used for the analysis of field samples as are used in annealing experiments, and subsequently employed in numerical models to predict thermal history. A parallel argument can be advanced for using samples of similar composition. Further, we recommend that the FT community should seek as a matter of some urgency a programme of interlaboratory comparison of track-length measurement using

* Corresponding author. Tel.: +44-20-7679-7704; fax: +44-20-7813-2802.
*E-mail address:* t.hurford@ucl.ac.uk (T. Hurford).
[1] Present address: Laboratoire de Géochimie, Bâtiment 504, Université Paris Sud, F-91405 Orsay-Cedex, France.


doi:10.1016/S0009-2541(02)00423-0

standard apatite samples containing artificial length distributions typifying various levels of complexity. Such comparisons would provide a more rigorous baseline for thermal history prediction in geological case studies.


*Keywords:* Apatite fission-track analysis; Confined track length; Methodology; Thermal history modelling; Interlaboratory standardisation

## 1. Introduction and objectives

Apatite Fission-Track (FT) thermochronology is widely used for reconstruction of low-temperature (<110 °C) thermal history in upper crustal rocks. The method has found particular application in estimating temperature history and long-term denudation rates in orogenic belts, rifted margins and more stable areas, providing a mean of assessing the timing and volume of sediment being delivered to sedimentary basins, and as an estimator of hydrocarbon maturity potential (Green et al., 1989a; Gallagher et al., 1994; Fitzgerald et al., 1995; Carter, 1999).

The proliferation of FT laboratories and abundance of published FT applications testifies to the apparent versatility and ubiquitous value of the method. Analysis requires the dual measurement of FT age and track length. Apatite *FT age* is given by the proportion of fissioned uranium atoms per unit area. The resulting tracks accumulate over time and are semi-stable: each track will shorten or anneal according to the maximum temperature it has experienced. *Track length* thus records temperature, and provides the key to understanding the FT age and deciphering the integrated sample thermal history (e.g. Gleadow et al., 1986).

The foundation stone for thermal history measurement is the measurement of track-length reduction in samples heated in a laboratory furnace, supplemented by length measurements in geological case studies where time–temperature history may be reasonably inferred (Green et al., 1986; Crowley et al., 1991; Carlson et al., 1999). Upon this annealing database are constructed algorithms which describe the time and temperature dependency of the track annealing process (Laslett et al., 1987; Crowley et al., 1991; Galbraith and Laslett, 1996; Ketcham et al., 1999). Extension of isothermal laboratory annealing data to variable temperature annealing and extrapolation to geological time periods (Duddy et al., 1988; Green et al., 1989b) has enabled the use of these annealing descriptions in numerical models to predict FT lengths and ages for a specific time–temperature scenario, which may be compared with real FT values measured for a field sample (Lutz and Omar, 1991; Gallagher, 1995; Willett, 1997; Ketcham et al., 1999). In a geological application, maximum palaeotemperatures, periods of heating and cooling, estimates of the amount and timing of missing section, denudation amounts and rates, "uplift"...all are postulated from the goodness-of-fit of such predictions with measured sample FT data, constrained by other geological information.

An IUGS recommendation on a standardised approach to *FT age calibration* was accepted by FT workers in 1988 (Hurford, 1990). This has generated a degree of transparency in subsequent age datasets, and permitted confident comparison of results from different workers and laboratories. Standardisation of track-length measurement has been treated much less rigorously. A pilot interlaboratory study presented at the Philadelphia FT workshop in 1992 found variation between laboratories and analysts to be significantly greater than estimated uncertainties (Miller et al., 1993), although no explanation was given by the authors for the underlying causes of this variation. Since measurement of track length is the prime factor in assessing thermal history, and hence deriving a geological interpretation, it is critical that the cause and extent of such experimental variation is defined.

While much debate has centred, quite properly, on the influence of apatite composition on the rate of FT annealing and hence the prediction of thermal history (Green, 1995; Gallagher et al., 1998; Ketcham, 2000; Barbarand and Pagel, 2001), relatively scant attention has been paid to other fundamental sources of variation integral to track-length revelation, observation and measurement techniques.

Such variations pose important questions for apatite FT thermochronometry:

- are the uncertainties calculated for a track-length dataset reasonable estimates of the actual variation in the analysis process?

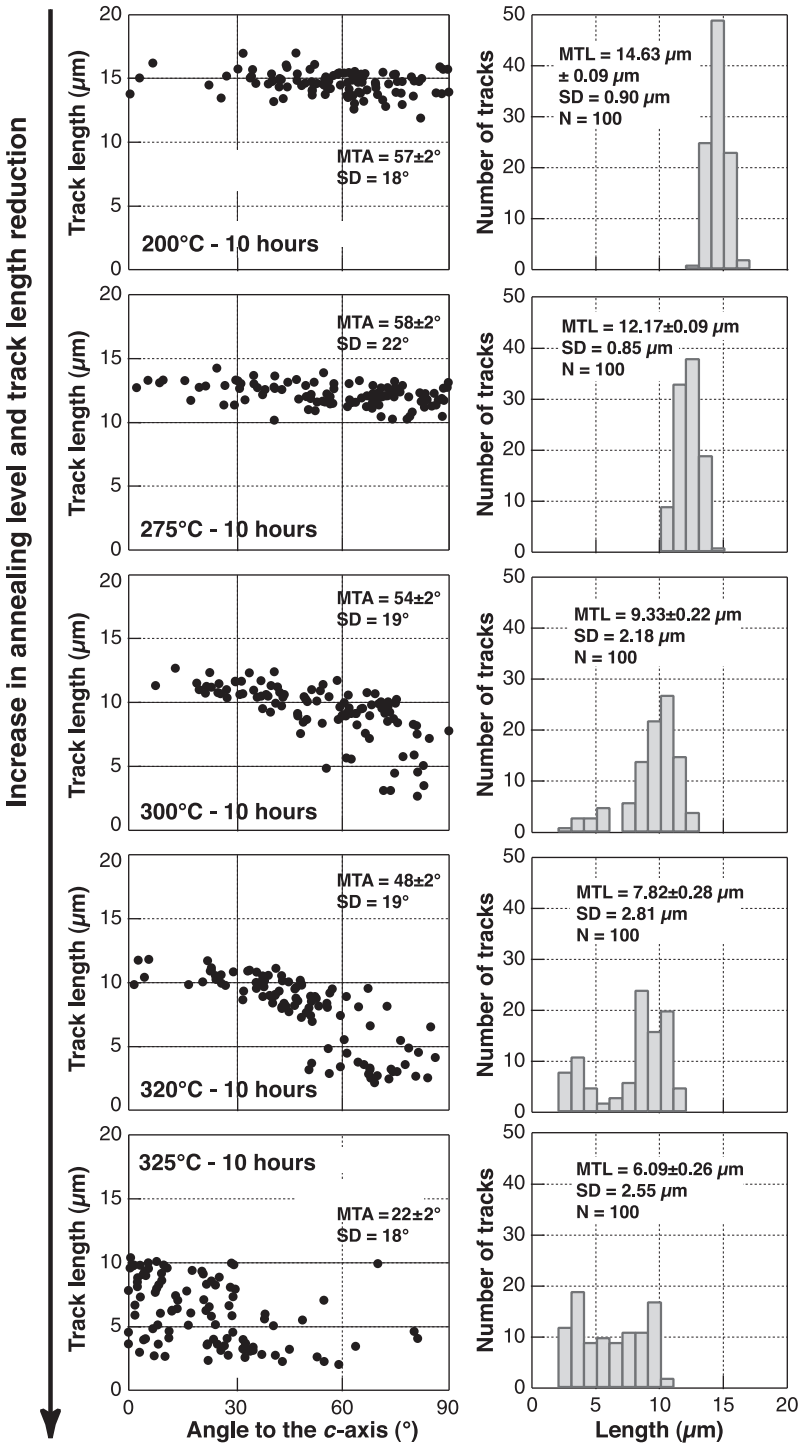


Fig. 1. Relationship between track length and angle to the *c*-axis for aliquots of a single fluor-apatite sample annealed at increasing temperatures for 10-h intervals. Sample etched 5 M $HNO_3$, 20 ± 1 °C, 20 s; TINTs only; single analyst.

- how confidently can track-length data from one worker or laboratory be compared with that of another worker or laboratory?
- how valid is it for an annealing model formulated in one laboratory under specific analytical conditions, to be used by analysts in another laboratory?

This latter question is of prime importance. For most FT analysts, geological interpretation of their FT sample data is derived by comparison with track-annealing data measured by other workers, in other laboratories, probably using different techniques and measurement criteria. Any differences resulting from variations in technique between the original annealing studies and a geological case study carried out in another laboratory will propagate directly into the sample FT results and hence into the modelled thermal history and geological interpretation. (Note that this applies equally to comparison of data from apatites of varying composition—see Hegarty, 2000.) Frequently, no assessment of such uncertainties is made and indeed analysts may not be aware that such sources of variation exist.

Answering these three questions is the ultimate objective of our studies. The specific purpose of this contribution is to examine further the extent of variation in track-length data, to examine the sources of such variation, and to derive a first measure of their magnitude. In the same way that age standards and the zeta calibration approach have provided rigour for FT age measurement (Fleischer and Hart, 1972; Hurford and Green, 1983; Hurford, 1990), we discuss briefly the possible use of FT length "standards" to facilitate interlaboratory comparison of track-length data and hence derive a more robust baseline for thermal history prediction. Variation in track-length measurement will influence mean track length and the length distribution, and thus directly affect the reconstruction of geological thermal history.

## 2. Definitions and experimental

As with most analysts, we favour certain techniques based on experience, personal and published experimental evidence, and anecdotal report. During

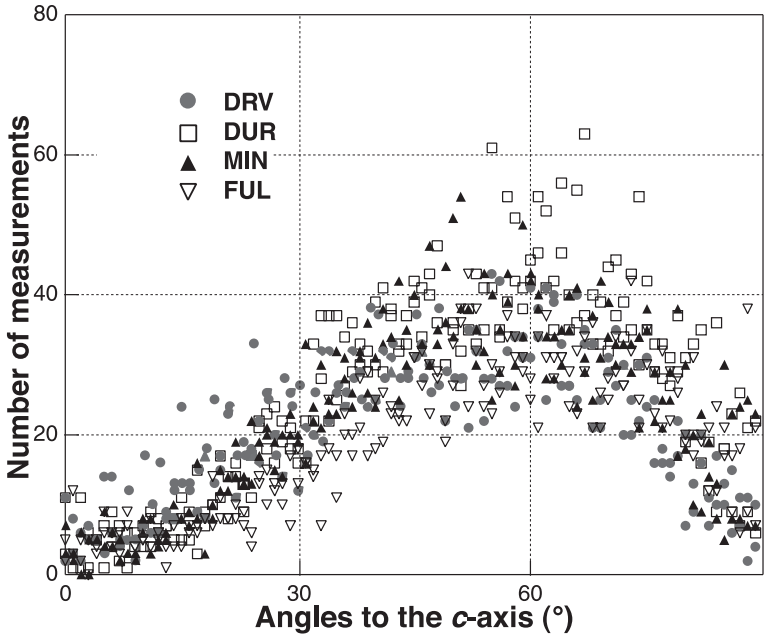


Fig. 2. Distribution of numbers of track lengths relative to angle to the *c*-crystallographic axis (in 1° bins), measured in aliquots of four apatites of varying composition exposed to different levels of annealing. Samples etched 5 M $HNO_3$, 20 ± 1 °C, 20 s; TINTs only.

preparation for an extensive laboratory study in the London laboratory of FT annealing in apatites with varying anion and cation composition (Barbarand et al., submitted for publication), we questioned our preferences, revisiting published techniques and concepts, and conducting a series of carefully planned experiments to test our methodology. We have used apatite aliquots from this annealing study to test track-length variation: these have been selected to give a broad range of track lengths and length distributions. The exact conditions of laboratory annealing are not relevant to this paper but are noted in the table captions. Further specific detail can be sourced by cross-referencing to our companion paper (Barbarand et al., submitted for publication).

In this study, we define track length as horizontal confined track length (Laslett et al., 1982) and track angle as the angle of an horizontal confined track to the *c*-crystallographic axis. Mean track length is denoted MTL and mean track angle MTA. Unless otherwise stated, all tracks were etched using 5 M $HNO_3$ at $20 \pm 1$ °C for 20 s (see Section 6.1), all measurements are track-in-track (TINT) (see Section 6.2) and uncertainties are shown as $\pm 1$ standard error of the mean (S.E.M.). Measurements were made only on prismatic sections, characterised by elongated etch pits parallel to the *c*-axis where etching effi-

Table 1
Replicate measurement of track length and track angle in the same apatite mounts by the same analyst after a 3-month interval

| Sample | 1st Analysis | | | | | 2nd Analysis | | | | |
|---|---|---|---|---|---|---|---|---|---|---|
| | MTL (μm) ± 1 S.E.M. | ± 1 S.D. | *N* | MTA (°) ± 1 S.E.M. | ± 1 S.D. | MTL (μm) ± 1 S.E.M. | ± 1 S.D. | *N* | MTA (°) ± 1 S.E.M. | ± 1 S.D. |
| FCT200B | 15.30 ± 0.08 | 0.85 | 102 | 56 ± 2 | 19 | 15.20 ± 0.08 | 0.82 | 102 | 58 ± 2 | 18 |
| DUR200B | 15.04 ± 0.09 | 0.90 | 101 | 55 ± 2 | 17 | 14.98 ± 0.08 | 0.80 | 101 | 56 ± 2 | 15 |
| BAM240B | 14.72 ± 0.09 | 0.90 | 103 | 51 ± 2 | 21 | 14.92 ± 0.09 | 0.85 | 101 | 54 ± 2 | 21 |
| MIN240B | 14.50 ± 0.07 | 0.68 | 103 | 55 ± 2 | 19 | 14.56 ± 0.08 | 0.76 | 102 | 54 ± 2 | 19 |
| GUN280B | 14.46 ± 0.07 | 0.72 | 102 | 52 ± 2 | 21 | 14.36 ± 0.08 | 0.77 | 101 | 55 ± 2 | 20 |
| UMB240B | 14.27 ± 0.08 | 0.81 | 103 | 57 ± 2 | 20 | 14.20 ± 0.06 | 0.61 | 101 | 64 ± 2 | 17 |
| DRV240B | 14.22 ± 0.08 | 0.85 | 102 | 57 ± 2 | 18 | 14.11 ± 0.09 | 0.85 | 101 | 61 ± 2 | 17 |
| DUR240B | 14.14 ± 0.08 | 0.78 | 103 | 58 ± 2 | 16 | 14.16 ± 0.07 | 0.69 | 101 | 57 ± 2 | 16 |
| GIL240B | 14.03 ± 0.07 | 0.74 | 102 | 52 ± 2 | 23 | 13.72 ± 0.09 | 0.86 | 83 | 51 ± 2 | 21 |
| WIL240B | 13.51 ± 0.08 | 0.78 | 102 | 61 ± 2 | 15 | 13.76 ± 0.07 | 0.73 | 101 | 57 ± 2 | 16 |
| FUL275B | 13.24 ± 0.07 | 0.68 | 102 | 59 ± 2 | 16 | 13.30 ± 0.06 | 0.65 | 101 | 59 ± 2 | 15 |
| FUL300B | 12.64 ± 0.09 | 0.86 | 103 | 60 ± 2 | 15 | 12.67 ± 0.08 | 0.83 | 102 | 55 ± 2 | 18 |
| DRV275B | 12.26 ± 0.09 | 0.86 | 101 | 58 ± 2 | 16 | 12.57 ± 0.08 | 0.83 | 102 | 57 ± 2 | 17 |
| FAR280B | 11.55 ± 0.09 | 0.89 | 102 | 54 ± 2 | 21 | 11.78 ± 0.09 | 0.90 | 101 | 53 ± 2 | 22 |
| DUR300B | 11.09 ± 0.07 | 0.74 | 102 | 60 ± 2 | 17 | 10.88 ± 0.08 | 0.84 | 103 | 53 ± 2 | 18 |
| MIN312B | 10.40 ± 0.11 | 1.07 | 103 | 48 ± 2 | 18 | 10.68 ± 0.13 | 1.31 | 100 | 45 ± 2 | 18 |
| UMB312B | 10.39 ± 0.09 | 0.94 | 100 | 55 ± 2 | 21 | 10.42 ± 0.13 | 1.08 | 71 | 56 ± 2 | 21 |
| DUR325B | 9.24 ± 0.19 | 1.90 | 102 | 44 ± 2 | 19 | 9.29 ± 0.21 | 2.08 | 100 | 41 ± 2 | 18 |
| DUR320B | 8.82 ± 0.26 | 2.56 | 101 | 50 ± 2 | 22 | 8.62 ± 0.22 | 2.23 | 101 | 51 ± 2 | 21 |
| DUR295C | 8.50 ± 0.23 | 2.34 | 101 | 47 ± 2 | 19 | 8.45 ± 0.25 | 2.52 | 102 | 48 ± 2 | 19 |
| MIN325B | 8.21 ± 0.24 | 2.46 | 103 | 46 ± 2 | 19 | 8.81 ± 0.23 | 2.35 | 100 | 42 ± 2 | 21 |
| GUN360B | 8.20 ± 0.23 | 2.44 | 109 | 48 ± 2 | 23 | 7.85 ± 0.25 | 2.58 | 103 | 50 ± 2 | 24 |
| MIN320B | 8.18 ± 0.26 | 2.62 | 102 | 45 ± 2 | 18 | 8.57 ± 0.23 | 2.31 | 100 | 47 ± 2 | 20 |
| MIN295C | 7.90 ± 0.30 | 3.01 | 101 | 42 ± 2 | 22 | 8.30 ± 0.25 | 2.47 | 100 | 43 ± 2 | 18 |
| UMB325B | 7.35 ± 0.25 | 2.48 | 102 | 55 ± 2 | 23 | 8.39 ± 0.25 | 2.51 | 100 | 49 ± 2 | 21 |
| FAR300B | 6.93 ± 0.39 | 3.23 | 70 | 52 ± 2 | 21 | 8.16 ± 0.36 | 2.78 | 62 | 49 ± 2 | 21 |
| WIL320B | 6.50 ± 0.33 | 3.37 | 103 | 52 ± 2 | 20 | 6.98 ± 0.33 | 3.29 | 100 | 52 ± 2 | 20 |
| DRV287C | 5.67 ± 0.30 | 3.06 | 101 | 37 ± 2 | 16 | 5.64 ± 0.30 | 3.07 | 104 | 36 ± 2 | 16 |

Samples contain induced tracks, partially annealed during laboratory experiments; sample number identifies annealing temperature in °C and time, where $B = 10$ h and $C = 100$ h; see Barbarand et al., submitted for publication for more details. Samples etched 5 M $HNO_3$ $20 \pm 1$ °C 20 s. TINTs only measured.

ciency is high and a geometry factor of 0.5 appropriate (Gleadow et al., 1986). Horizontal tracks were recognised using reflected light, with most measurements made in transmitted light. All measurements used Zeiss Axioplan microscopes (100 × dry objective, 1250 × total magnification), linked via a drawing tube to a computer-controlled Houston Instruments digitising tablet with a small LED in the centre of its cursor. Repeated calibration before each measurement used a Graticules 1-mm stage micrometer with 2-μm divisions; precision of the measuring system (assessed from repeated analyses, each taking 100 measurements, of a 20-μm scale bar) is estimated at ± 0.11 μm (>99%). Track angle was measured for each track by recording three sets of *X*,*Y* co-ordinates, at either end of the track and along the *c*-axis from one track end. Repeat measurements used the same sample mounts, but not necessarily the same areas or tracks.

## 3. Relationship of track length and angle

Observed and measured distributions of confined track lengths in apatite are anisotropic and strongly controlled by the track orientation relative to the crystallographic *c*-axis. Anisotropy of etching (see Section 6) may result in preferential revelation of tracks at higher angles to the *c*-axis. Annealing is also anisotropic with tracks at high angles to the *c*-axis annealing more rapidly than those tracks parallel to the *c*-axis (Green and Durrani, 1977). This anisotropy increases with annealing (see Green, 1981; Laslett et al., 1984; Green et al., 1986; Donelick et al., 1990; Galbraith et al., 1990; Donelick, 1991; Donelick et al., 1999). The evolution of the track length and angle relationship with increased annealing is illustrated in Fig. 1. For long MTLs (>13 μm), tracks are of similar length, within error, irrespective of track orientation. As annealing increases, the MTL is reduced with tracks perpendicular to the *c*-axis shortening at a faster rate than tracks at lower angles. For samples with mean track lengths < 9 μm, a distinct bimodal length distribution can be discerned: tracks sub-parallel to the *c*-axis range between 8 and 13 μm, while tracks perpendicular to the *c*-axis vary between 2 and 7 μm. In weakly and moderately annealed samples, MTAs range between 48° and 65° while for very strongly annealed samples, MTAs range between 15° and 25°.

Fig. 2 emphasises this non-uniform distribution. For each of four apatites, the numbers of track lengths measured in aliquots exposed to all levels of annealing are summed in 1° bins. Irrespective of apatite composition, the distribution is negatively skewed with the mode around 60°, higher than the theoretical value of 45° if tracks were uniformly distributed, revealed and observed. Such a non-uniform distribution results in part from anisotropic track annealing and track etching but other factors contribute. An orientation bias may also be introduced by the shape of the host semi-track (or surface track) (Galbraith et al., 1990): the probability of intersecting (and thus of etching) a track perpendicular to the *c*-axis is greater because the semi-track host offers a wider face to that direction. Observer bias also produces anisotropy. Tracks perpendicular to the *c*-axis are easier to recognise and thus are measured in higher proportion. High track densities and the use of reflected light favours observation and measurement of high-angle tracks. Thin

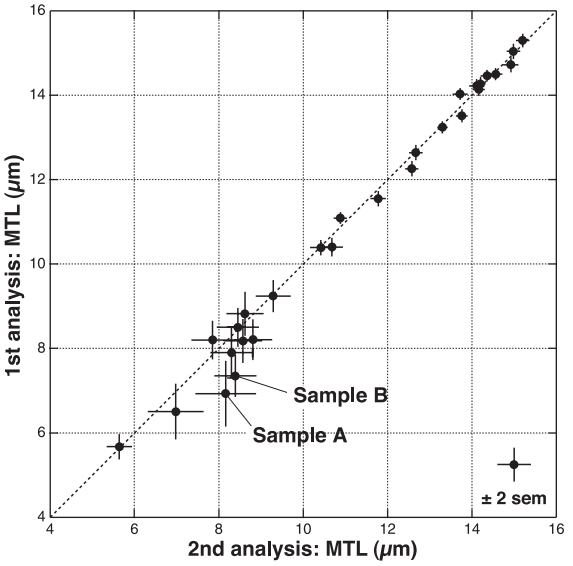


Fig. 3. Replicate measurement of track length in a variety of apatite samples made by a single analyst after a 3-month interval. Samples contain induced tracks, partially annealed during laboratory experiments. Samples etched 5 M $HNO_3$, 20 ± 1 °C, 20 s; TINTS only; ~ 100 tracks per measurement. Length vs. angle plots for samples A and B shown in Fig. 4.

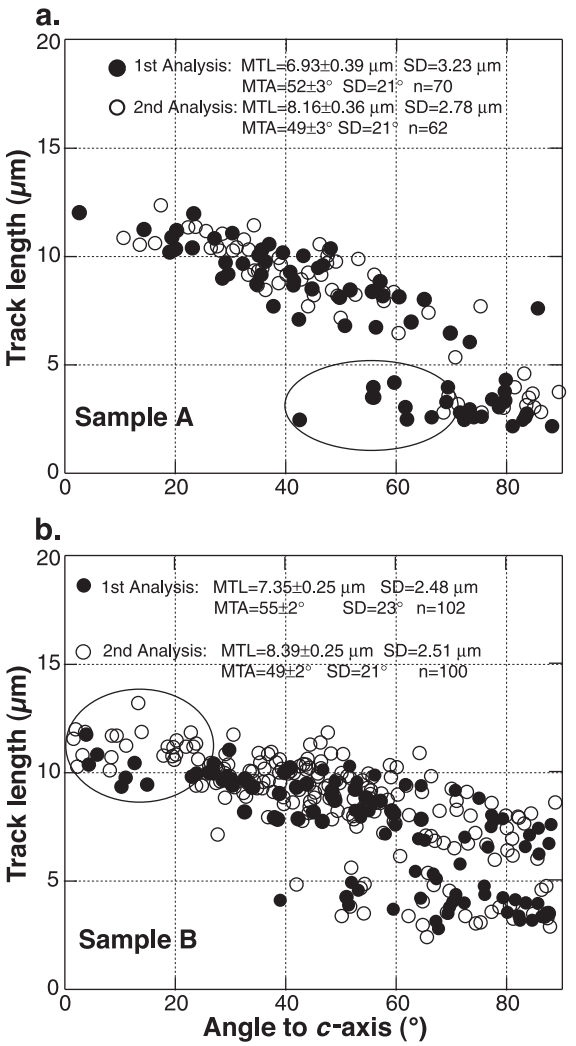


Fig. 4. Relationship between track length and angle to *c*-axis for two apatite samples in Fig. 3 where replicate measurements show large variation. Ellipses indicate probable sources of variation (see text). Sample A = FAR300B; sample B = UMB325B. Samples etched 5 M $HNO_3$, 20 ± 1 °C, 20 s; TINTs only; single analyst.

tracks (low-angle tracks) are more difficult to observe with reflected light. Strangely, under conditions of strong annealing (MTLs < 10 µm), anisotropy from observer bias may be less of a problem because analysis technique can change, possibly becoming more rigorous: because there are few TINTs the analyst looks harder to find any or all confined tracks, irrespective of orientation.

## 4. Reproducibility of analysis

Two aspects of variation in track-length measurement are important: the consistency of a single analyst and comparability of results between different analysts. Each of these may vary depending on the complexity of the sample under analysis. Published data testing these fundamental variations are few and diffuse.

Gleadow et al. (1986) compared measurements (some using an eye-piece scale bar) made by different observers on induced and volcanic-type spontaneous track lengths in a range of apatites. They concluded that differences of ~ 0.3 µm probably result from individual preferences in measurement including subdivision of the scale-bar interval. Green et al. (1986) also compared measurements on the same samples

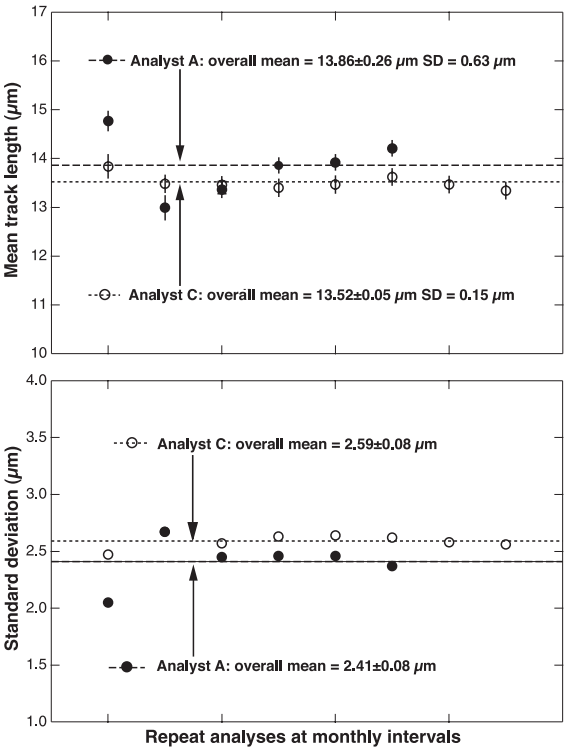


Fig. 5. Replicate measurement of MTL in same apatite sample by two analysts at monthly intervals. Overall mean of each analyst shown by dashed lines. Sample contains induced tracks partially annealed and reirradiated to give an artificial bimodal distribution. Samples etched 5 M $HNO_3$, 20 ± 1 °C, 20 s; TINTs only; ~ 100 tracks per measurement. Error bars are ± 1 standard error.

Table 2
Length and angle measurements in the same apatite mounts by three different analysts

| Sample | Analyst A | | | | | Analyst B | | | | | Analyst C | | | | |
|---|---|---|---|---|---|---|---|---|---|---|---|---|---|---|---|
| | MTL (μm) ± 1 S.E.M. | ±1 S.D. | *N* | MTA (°) ± 1 S.E.M. | ±1 S.D. | MTL (μm) ± 1 S.E.M. | ±1 S.D. | *N* | MTA (°) ± 1 S.E.M. | ±1 S.D. | MTL (μm) ± 1 S.E.M. | ±1 S.D. | *N* | MTA (°) ± 1 S.E.M. | ±1 S.D. |
| BAM240B | 14.98 ± 0.09 | 0.85 | 100 | 53 ± 2 | 22 | 14.87 ± 0.09 | 0.94 | 102 | 56 ± 2 | 20 | 14.72 ± 0.09 | 0.90 | 103 | 51 ± 2 | 21 |
| MIN240B | 14.22 ± 0.09 | 0.90 | 100 | 60 ± 2 | 20 | 14.39 ± 0.09 | 0.88 | 102 | 58 ± 2 | 19 | 14.50 ± 0.07 | 0.68 | 103 | 55 ± 2 | 19 |
| UMB240B | 14.19 ± 0.07 | 0.71 | 100 | 57 ± 2 | 20 | 14.09 ± 0.09 | 0.91 | 103 | 62 ± 2 | 20 | 14.27 ± 0.08 | 0.81 | 103 | 57 ± 2 | 20 |
| DUR240B | 14.07 ± 0.09 | 0.85 | 100 | 61 ± 2 | 17 | 14.06 ± 0.07 | 0.78 | 113 | 58 ± 2 | 17 | 14.14 ± 0.08 | 0.78 | 103 | 58 ± 2 | 16 |
| GIL240B | 14.02 ± 0.09 | 0.86 | 100 | 61 ± 2 | 22 | 13.97 ± 0.10 | 0.95 | 96 | 58 ± 2 | 22 | 14.03 ± 0.07 | 0.74 | 102 | 52 ± 2 | 23 |
| FUL280B | 13.86 ± 0.09 | 0.93 | 100 | 55 ± 2 | 19 | 13.44 ± 0.08 | 0.84 | 107 | 60 ± 2 | 20 | 13.86 ± 0.07 | 0.75 | 104 | 54 ± 2 | 19 |
| BAM275B | 13.83 ± 0.10 | 0.99 | 100 | 55 ± 2 | 23 | 13.85 ± 0.10 | 0.97 | 101 | 56 ± 2 | 22 | 13.57 ± 0.10 | 0.97 | 102 | 57 ± 2 | 19 |
| LIN275B | 13.83 ± 0.13 | 0.99 | 56 | 59 ± 3 | 19 | 13.86 ± 0.13 | 0.87 | 43 | 51 ± 3 | 23 | 13.99 ± 0.21 | 1.02 | 24 | 52 ± 4 | 20 |
| BAM280B | 13.81 ± 0.09 | 0.90 | 100 | 54 ± 2 | 22 | 12.94 ± 0.10 | 1.00 | 101 | 56 ± 2 | 19 | 13.53 ± 0.11 | 1.09 | 103 | 47 ± 2 | 20 |
| DRV240B | 13.72 ± 0.07 | 0.71 | 101 | 61 ± 2 | 18 | 13.96 ± 0.08 | 0.85 | 103 | 56 ± 2 | 17 | 14.22 ± 0.08 | 0.85 | 102 | 57 ± 2 | 18 |
| UNK240B | 13.48 ± 0.08 | 0.78 | 100 | 57 ± 2 | 23 | 13.60 ± 0.09 | 0.74 | 75 | 51 ± 3 | 23 | 13.25 ± 0.13 | 0.87 | 45 | 60 ± 3 | 19 |
| FUL275B | 13.36 ± 0.08 | 0.84 | 100 | 60 ± 2 | 23 | 13.69 ± 0.09 | 0.90 | 103 | 61 ± 1 | 15 | 13.24 ± 0.07 | 0.68 | 102 | 59 ± 2 | 16 |
| WIL240B | 13.34 ± 0.08 | 0.75 | 100 | 61 ± 2 | 16 | 13.36 ± 0.08 | 0.87 | 107 | 56 ± 2 | 17 | 13.51 ± 0.08 | 0.78 | 102 | 61 ± 1 | 15 |
| GUN300B | 13.18 ± 0.08 | 0.82 | 100 | 56 ± 2 | 21 | 13.07 ± 0.11 | 1.09 | 101 | 61 ± 2 | 18 | 13.49 ± 0.08 | 0.83 | 102 | 53 ± 2 | 21 |
| UMB280B | 13.18 ± 0.10 | 1.01 | 100 | 54 ± 2 | 20 | 13.08 ± 0.09 | 0.90 | 103 | 57 ± 2 | 20 | 13.11 ± 0.09 | 0.87 | 100 | 54 ± 2 | 20 |
| UMB275B | 13.11 ± 0.10 | 1.03 | 101 | 58 ± 2 | 20 | 13.12 ± 0.08 | 0.83 | 101 | 60 ± 2 | 18 | 13.19 ± 0.09 | 0.88 | 102 | 56 ± 2 | 18 |
| BAM300B | 13.03 ± 0.11 | 1.06 | 100 | 52 ± 2 | 21 | 12.80 ± 0.10 | 0.96 | 100 | 54 ± 2 | 21 | 12.66 ± 0.10 | 0.95 | 101 | 49 ± 2 | 22 |
| MIN280B | 12.88 ± 0.10 | 1.03 | 100 | 59 ± 2 | 23 | 12.70 ± 0.08 | 0.83 | 103 | 58 ± 2 | 15 | 12.55 ± 0.08 | 0.85 | 102 | 58 ± 1 | 15 |
| MIN275B | 12.80 ± 0.10 | 1.02 | 100 | 59 ± 2 | 19 | 12.59 ± 0.10 | 1.06 | 103 | 56 ± 2 | 20 | 12.38 ± 0.13 | 1.25 | 95 | 47 ± 2 | 18 |
| DUR280B | 12.71 ± 0.11 | 1.05 | 100 | 57 ± 2 | 18 | 11.94 ± 0.09 | 0.92 | 103 | 57 ± 1 | 14 | 12.57 ± 0.09 | 0.95 | 103 | 59 ± 2 | 16 |
| LIN310B | 12.69 ± 0.14 | 1.37 | 100 | 53 ± 3 | 25 | 12.68 ± 0.11 | 1.08 | 100 | 58 ± 2 | 21 | 13.13 ± 0.10 | 1.04 | 100 | 53 ± 2 | 23 |
| GUN320B | 12.65 ± 0.10 | 0.99 | 100 | 58 ± 2 | 20 | 12.64 ± 0.09 | 0.91 | 104 | 57 ± 2 | 20 | 12.71 ± 0.09 | 0.87 | 102 | 54 ± 2 | 20 |
| DUR275B | 12.64 ± 0.08 | 0.79 | 100 | 63 ± 2 | 19 | 13.22 ± 0.09 | 0.91 | 105 | 54 ± 2 | 20 | 12.34 ± 0.09 | 0.89 | 100 | 58 ± 2 | 18 |
| FUL300B | 12.55 ± 0.09 | 0.85 | 100 | 55 ± 2 | 21 | 12.42 ± 0.09 | 0.87 | 104 | 56 ± 2 | 17 | 12.64 ± 0.09 | 0.86 | 103 | 60 ± 2 | 15 |
| DRV275B | 12.45 ± 0.11 | 1.11 | 100 | 60 ± 2 | 18 | 12.44 ± 0.08 | 0.78 | 103 | 60 ± 2 | 17 | 12.26 ± 0.09 | 0.86 | 101 | 58 ± 2 | 16 |
| GIL275B | 12.44 ± 0.10 | 0.97 | 100 | 62 ± 2 | 21 | 12.31 ± 0.08 | 0.78 | 104 | 63 ± 2 | 19 | 12.42 ± 0.09 | 0.93 | 103 | 61 ± 2 | 20 |
| WIL275B | 12.17 ± 0.09 | 0.85 | 100 | 58 ± 2 | 22 | 12.18 ± 0.08 | 0.83 | 102 | 54 ± 2 | 19 | 12.23 ± 0.08 | 0.78 | 107 | 52 ± 2 | 19 |
| GIL280B | 12.06 ± 0.10 | 1.00 | 100 | 56 ± 2 | 22 | 12.08 ± 0.08 | 0.82 | 104 | 57 ± 2 | 19 | 12.12 ± 0.08 | 0.81 | 101 | 63 ± 2 | 18 |

| | | | | | | | | | | | | | | |
|---|---|---|---|---|---|---|---|---|---|---|---|---|---|---|
| FAR275B | 12.02 ± 0.10 | 1.03 | 100 | 58 ± 2 | 21 | 12.11 ± 0.10 | 0.99 | 101 | 52 ± 2 | 18 | 11.99 ± 0.09 | 0.94 | 102 | 53 ± 2 | 21 |
| UNK275B | 11.96 ± 0.09 | 0.90 | 100 | 57 ± 2 | 17 | 12.23 ± 0.07 | 0.74 | 101 | 57 ± 2 | 20 | 11.88 ± 0.11 | 1.08 | 94 | 56 ± 2 | 18 |
| BAM312B | 11.91 ± 0.12 | 1.22 | 101 | 53 ± 2 | 21 | 11.86 ± 0.12 | 1.22 | 100 | 56 ± 2 | 21 | 11.82 ± 0.12 | 1.18 | 101 | 55 ± 2 | 21 |
| MIN300B | 11.81 ± 0.10 | 0.96 | 100 | 61 ± 2 | 19 | 11.74 ± 0.09 | 0.90 | 102 | 56 ± 2 | 19 | 11.69 ± 0.09 | 0.93 | 102 | 56 ± 2 | 18 |
| BAM320B | 11.67 ± 0.13 | 1.34 | 100 | 47 ± 2 | 24 | 11.46 ± 0.11 | 1.13 | 103 | 47 ± 2 | 22 | 11.75 ± 0.12 | 1.22 | 102 | 45 ± 2 | 21 |
| WIL280B | 11.67 ± 0.09 | 0.90 | 100 | 61 ± 2 | 18 | 11.70 ± 0.08 | 0.82 | 105 | 58 ± 2 | 18 | 11.66 ± 0.08 | 0.81 | 102 | 57 ± 2 | 14 |
| UMB300B | 11.59 ± 0.13 | 1.15 | 82 | 60 ± 2 | 21 | 11.61 ± 0.12 | 1.02 | 73 | 61 ± 2 | 18 | 11.70 ± 0.11 | 0.92 | 69 | 57 ± 2 | 20 |
| DRV280B | 11.43 ± 0.11 | 1.11 | 100 | 61 ± 2 | 16 | 12.05 ± 0.09 | 0.88 | 103 | 57 ± 2 | 16 | 11.72 ± 0.10 | 0.98 | 103 | 58 ± 2 | 16 |
| UNK280B | 11.34 ± 0.10 | 1.02 | 100 | 60 ± 2 | 20 | 11.79 ± 0.08 | 0.83 | 102 | 59 ± 2 | 17 | 11.34 ± 0.09 | 0.91 | 94 | 54 ± 2 | 17 |
| BAM325B | 11.18 ± 0.14 | 1.35 | 100 | 58 ± 2 | 24 | 10.43 ± 0.13 | 1.33 | 103 | 59 ± 2 | 21 | 11.11 ± 0.11 | 1.15 | 101 | 52 ± 2 | 21 |
| DUR300B | 11.18 ± 0.11 | 1.05 | 100 | 56 ± 2 | 23 | 11.01 ± 0.11 | 1.13 | 101 | 58 ± 2 | 20 | 11.09 ± 0.07 | 0.74 | 102 | 60 ± 2 | 17 |
| FUL312B | 10.69 ± 0.26 | 1.52 | 34 | 47 ± 5 | 26 | 9.90 ± 0.29 | 0.87 | 10 | 60 ± 6 | 20 | 10.98 ± 0.27 | 0.94 | 13 | 48 ± 6 | 21 |
| DUR312B | 10.24 ± 0.14 | 1.37 | 102 | 56 ± 2 | 18 | 9.85 ± 0.11 | 1.13 | 99 | 57 ± 2 | 16 | 9.74 ± 0.15 | 1.47 | 103 | 52 ± 2 | 18 |
| DRV300B | 9.91 ± 0.14 | 1.37 | 100 | 54 ± 2 | 17 | 9.66 ± 0.15 | 1.48 | 102 | 52 ± 2 | 17 | 9.68 ± 0.20 | 2.01 | 102 | 54 ± 2 | 17 |
| GIL300B | 9.61 ± 0.18 | 1.78 | 100 | 56 ± 2 | 22 | 9.90 ± 0.13 | 1.30 | 102 | 53 ± 2 | 21 | 9.75 ± 0.14 | 1.46 | 103 | 56 ± 2 | 22 |
| WIL300B | 9.33 ± 0.22 | 2.18 | 100 | 54 ± 2 | 19 | 9.48 ± 0.14 | 1.40 | 100 | 56 ± 2 | 18 | 9.35 ± 0.21 | 2.10 | 101 | 54 ± 2 | 19 |
| UNK300B | 9.17 ± 0.23 | 2.14 | 88 | 52 ± 2 | 23 | 9.22 ± 0.20 | 1.91 | 89 | 49 ± 2 | 19 | 8.25 ± 0.28 | 2.82 | 101 | 54 ± 2 | 21 |
| DUR320B | 8.70 ± 0.23 | 2.30 | 100 | 53 ± 2 | 20 | 8.64 ± 0.21 | 2.12 | 101 | 53 ± 2 | 19 | 8.62 ± 0.22 | 2.23 | 101 | 51 ± 2 | 21 |
| UMB325B | 8.70 ± 0.21 | 2.14 | 100 | 49 ± 2 | 18 | 8.61 ± 0.19 | 1.86 | 101 | 50 ± 2 | 20 | 8.57 ± 0.17 | 2.36 | 200 | 49 ± 1 | 21 |
| DUR325B | 8.69 ± 0.24 | 2.40 | 100 | 46 ± 2 | 24 | 8.19 ± 0.23 | 2.34 | 103 | 45 ± 2 | 18 | 9.19 ± 0.15 | 2.14 | 200 | 41 ± 1 | 18 |
| FAR300B | 7.89 ± 0.30 | 3.00 | 101 | 54 ± 2 | 23 | 7.47 ± 0.26 | 2.63 | 100 | 50 ± 2 | 17 | 8.16 ± 0.36 | 2.78 | 62 | 49 ± 3 | 21 |
| WIL320B | 7.82 ± 0.28 | 2.81 | 100 | 48 ± 2 | 19 | 7.23 ± 0.27 | 2.70 | 101 | 48 ± 2 | 20 | 6.98 ± 0.33 | 3.29 | 100 | 52 ± 2 | 20 |
| GIL312B | 7.51 ± 0.26 | 2.62 | 100 | 31 ± 2 | 21 | 6.69 ± 0.24 | 2.40 | 103 | 34 ± 2 | 23 | 6.23 ± 0.28 | 2.80 | 101 | 38 ± 2 | 22 |
| DRV320B | 7.36 ± 0.23 | 2.27 | 100 | 24 ± 1 | 14 | 7.28 ± 0.21 | 2.14 | 101 | 29 ± 2 | 16 | 6.01 ± 0.35 | 2.63 | 57 | 32 ± 1 | 10 |
| WIL312B | 6.59 ± 0.30 | 3.00 | 100 | 49 ± 2 | 23 | 7.61 ± 0.25 | 2.40 | 96 | 39 ± 2 | 19 | 5.37 ± 0.30 | 2.97 | 100 | 46 ± 2 | 24 |
| DRV312B | 6.50 ± 0.28 | 2.79 | 100 | 42 ± 2 | 16 | 6.97 ± 0.20 | 1.99 | 101 | 38 ± 1 | 14 | 5.92 ± 0.29 | 2.93 | 101 | 41 ± 2 | 16 |
| DRV325B | 6.39 ± 0.22 | 2.23 | 100 | 21 ± 2 | 16 | 6.36 ± 0.21 | 2.08 | 101 | 22 ± 2 | 12 | 6.81 ± 0.22 | 2.20 | 101 | 20 ± 1 | 13 |

Samples contain induced tracks, partially annealed during laboratory experiments; see Barbarand et al., submitted for publication for more details. Samples etched 5 M $HNO_3$ 20 ± 1 °C 20 s. TINTs only measured.

made by two observers, finding a systematic difference of ~ 0.3–0.5 μm. Accordingly, they normalised the MTL measured by each observer to the respective mean length of unannealed tracks (*l*/*lo*). The track-length study of Miller et al. (1993) illustrated variation between observers in the case of two apatite samples with relatively simple, unimodal track-length distributions with supposed MTLs ~ 14.0 μm. Individual values ranged from 13.2 ± 0.1 to 14.7 ± 0.1 μm (sample 92-1) and 12.4 ± 0.2 to 14.1 ± 0.2 μm (sample 92-2); uncertainties are ± 1 S.E.M. Estimates of the spread of measured track-length values are provided by the standard deviations (1$\sigma$) which vary from 0.8 to 1.7 (sample 92-1) and from 1.0 to 2.4 μm (sample 92-2). No track angles were measured. This spread in data clearly exceeds individual measurement standard errors and, if propagated into a simple thermal history forward model with uniform burial and exhumation over 100 Ma, yields differences in predicted maximum palaeotemperature of >30 °C, equivalent to a denudation thickness of perhaps >1 km.

Carlson et al. (1999) have reported replicate analyses on individual fission-tracks citing measurement precisions of ± 0.15 μm and ± 2° for a single analyst. We have similarly replicated analysis of fission-track lengths in various apatite samples, selected because of the range of composition (see Appendix 1 in Barbarand et al., submitted for publication). An initial study compared repeat measurements by one analyst after a 3-month interval. Analysis was made of 28 aliquots of compositionally different apatites with a range of track-length distributions and MTLs varying between 15 and 6 μm, produced in 10- and 100-h annealing experiments (Table 1). Shown as a one-to-one plot in Fig. 3, 11 of the 28 analyses are not reproducible within ± 2 standard errors of the individual MTLs, with an apparent trend toward higher values for the second analysis period. The mean difference between the replicate analyses is 3%, but difference increases inversely with track length. Two samples (samples A and B in Fig. 3) deviate significantly from the plot (18% and 14% differences in measurement) and are characterised by short MTLs (< 9 μm) and bimodal length distributions resulting from very short tracks (< 5 μm) perpendicular to the *c*-axis. Plotting for each sample the angular distribution of tracks as a function of track length (Fig. 4) emphasises the interdependence of length and angle and underlines the angular anisotropy of annealing noted by Green and Durrani (1977) and considered further by Green et al. (1986) and Donelick (1991): tracks at high angles to the *c*-axis anneal more readily. Differences between the replicate measurements (Fig. 3) result from sampling bias. In sample (A), the shorter MTL in analysis #1 results from inclusion in the dataset of a cohort of shorter tracks in the mid-angle range (the ellipse in Fig. 4a); the resulting lower MTA of analysis #1 overlaps within one standard error with that of analysis #2. In sample (B), analysis #2 found more long tracks at low angles to the *c*-axis (the ellipse in Fig. 4b) and this is reflected more clearly in the different MTAs of the two measurements.

In a second study, two experienced analysts made monthly measurements of an artificial bimodal track-length distribution (Fig. 5). The same apatite sample was analysed each time, but the same areas were not specifically measured. Analyst C (open circles) demonstrates a high degree of consistency with five of eight analyses agreeing with his overall mean within one standard error of the individual analysis MTLs. Analyst A (filled circles) shows greater dispersion of results, with only two of six measurements agreeing with his overall mean within one standard error of the individual analysis MTLs. The overall difference in mean value between observers is only ~ 2%, but variation is nonsystematic on individual repeat measurements. Because this sample contains a bimodal length distribution, the simple comparison of MTLs misses the detail of the distribution which is the key record of thermal history and which is utilised in thermal history prediction (see, e.g. Gallagher, 1995). A plot of variation in length standard deviation shows a higher degree of consistency for analyst C, similar to the MTL results. The generally shorter MTLs of analyst C are accompanied by larger SDs, indicating that C is measuring more short tracks than analyst A. Measurement #1 yielded an anomalously high MTL for analyst A with a low SD: few short tracks were measured and analyst A recorded that this analysis "was made in a hurry".

A third study compared track-lengths measured in partially annealed, compositionally different apatites by three experienced analysts. The results (Table 2) show significant variation between observers, but

these are neither systematic nor specific to any individual: where one analyst is higher for one measurement, they may be lower than, or equal to the mean for others. Fig. 6 summarises this variation plotting the MTL residual for each analyst against the average MTL; both positive and negative residuals are shown. (Note the residual is the difference of each analyst's value from the average MTL value.) For comparison, the shaded areas correspond to one and two standard error values typical of one observer's MTL values, i.e. the uncertainty that would be reported for normal analysis by one observer.

As with the results found for one analyst, the level of scatter in the data increases towards shorter track lengths:

- for tracks >14 μm, little difference exits between analysts with a typical individual MTL standard error of 0.07–0.10 μm;
- for MTLs of 9–14 μm, clear differences exist between analysts with a typical individual MTL standard error of 0.10–0.20 μm;
- for MTLs <9 μm, large differences >1 μm may exist between observers, with a mean difference of ~ 0.35 μm.

Some systematic differences may be present at shorter lengths where analyst A finds longer MTLs more frequently, while analyst C reports shorter values. Clearly, ± values estimated and reported for MTLs, invariably at one standard error, substantially underestimate differences between analysts, especially at shorter lengths and perhaps two standard errors offer a more realistic assessment of observer variation.

The specific comparison of measurements by four analysts of one bimodal length distribution is given in Fig. 7. MTL values vary by up to 12%, the three values overlapping within one standard error, with the MTL of analyst A being significantly higher. While the more informative length distributions show broad similarity, clear differences do exist: analyst A has a high long/short track ratio which is less pronounced in analysts B and D. Analyst C recorded short tracks as

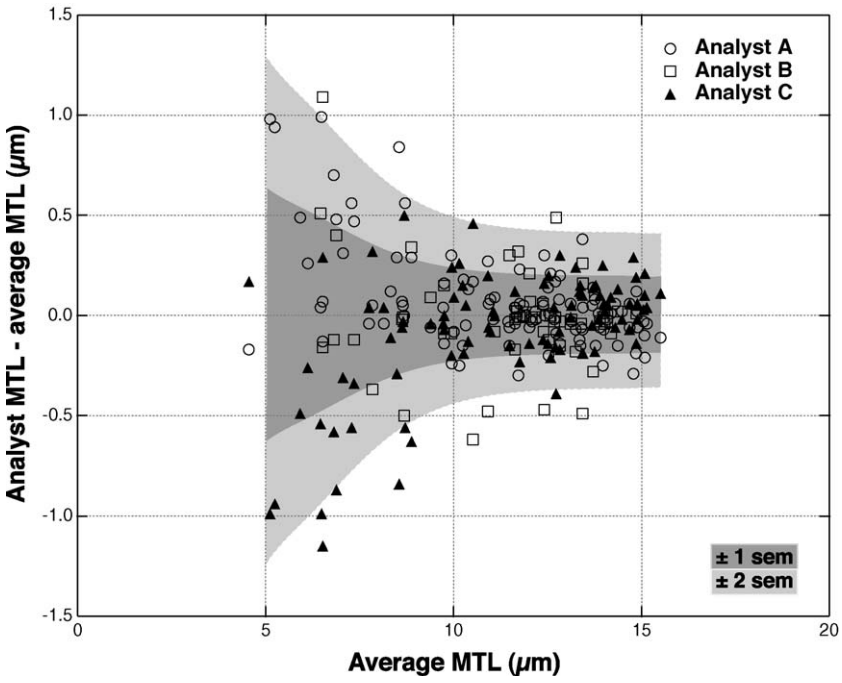


Fig. 6. Variation in track-length measurement between analysts. Grey areas correspond to one and two standard errors of the mean ( ± 1 and 2 S.E.M.) for the individual measurements with the largest standard errors. See text for further explanation.

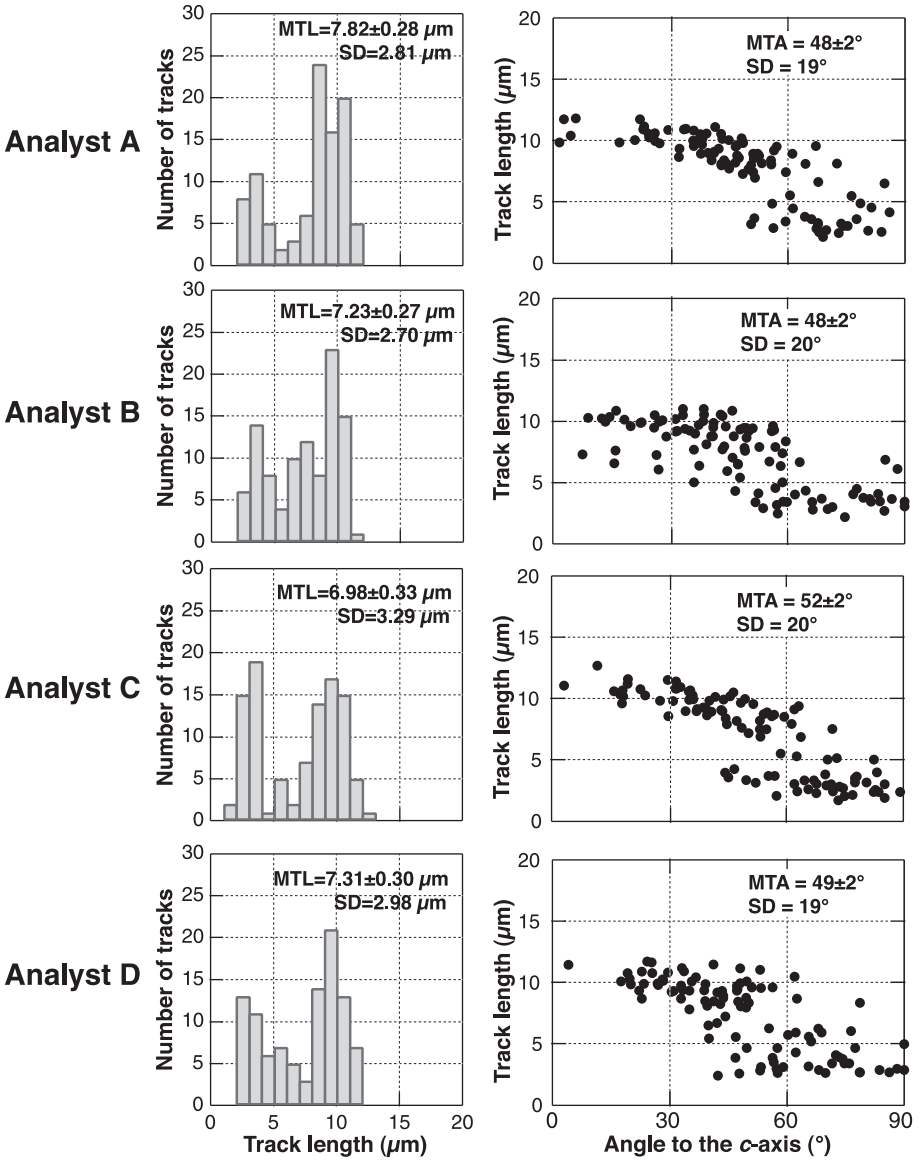


Fig. 7. Length and angle measurement of the same apatite samples by four different analysts. Sample contained induced tracks, partially annealed in laboratory experiments. Samples etched 5 M $HNO_3$, 20 ± 1 °C, 20 s. TINTs only measured, 100 tracks per analyst.

the primary mode. Variations in angle also exist; although MTA is an insufficiently sensitive measure to define this, the length/angle plots in Fig. 7 provide a qualitative indicator. Clearly, even for experienced analysts using the same equipment to measure the same sample, there is observer bias in sampling both length and angle.

## 5. Sources of variation

The above examples of replication of track-length measurement suggest that for a single analyst, differences in results are typically ~ 3%, but can rise to 18%; for measurement of the same samples by different experienced analysts typical variation is ~ 5%,

but in extreme cases can be ~ 30%. Although track lengths were of varying complexity, this may represent a best-case scenario with measurement using the same equipment and techniques. The 11–14% variation reported by Miller et al. (1993) represented different analysts with different techniques but on straightforward length distributions. Multi-analyst measurement of samples with shorter track lengths and complex distributions could exacerbate this variation.

Where does this variation arise? Laslett et al. (1982) have discussed bias in length measurement, recommending analysis of horizontal confined tracks on prismatic sections where bias may be reasonably inferred—see Section 2. Donelick and Miller (1991) have also attempted to explain differences between analysts. Drawing in part on their comments, certain potential sources of variation can be identified, some systematic, others nonsystematic.

Variation from track revelation:

- Apatite solubility controls the size and shape of tracks and is a function of apatite composition and etchant. Different etchants produce differing degrees of anisotropy; initial track length is also dependent on solubility.
- The two types of confined track "TINTs" and "TINCLEs" used in analysis have different biases.
- The use of $^{252}$Cf fission fragments to increase the number of etched and measured confined tracks may also introduce a bias.

Bias in measurement:

- Measurement biases are mainly systematic relating to the equipment and procedures used.
- Sample size directly affects precision and is especially important where track-length distributions are complex.

Observer bias: Observer biases are largely nonsystematic and relate to differences in, and consistency of personal technique. Carefulness, analysis time and conditions available, pressure of workload, tiredness. . .all can affect the efficacy of a manual FT analysis and introduce variation which is difficult to assess.

Variation between the analyses of a single operator and between measurements of different observers will be compounded from multiple sources, some systematic, others random. We next attempt to assess the possible contribution of some of these sources.

## 6. Track revelation

### 6.1. Track etching

Optical observation and measurement of fission-track lengths requires enlargement of the latent track through chemical etching, in apatite by using dilute $HNO_3$ at room temperature for a few seconds. Such etching (solubility) is controlled by the crystallographic properties of a mineral. Etching in apatite is anisotropic, with the general etch rate parallel to the *c*-axis being more rapid than that normal to it. This is reflected in the shape, length and distribution of the FT etch pits lying at different angles relative to the *c*-crystallographic axis (Gleadow, 1981; Singh et al., 1986; Donelick et al., 1990): tracks parallel to the *c*-

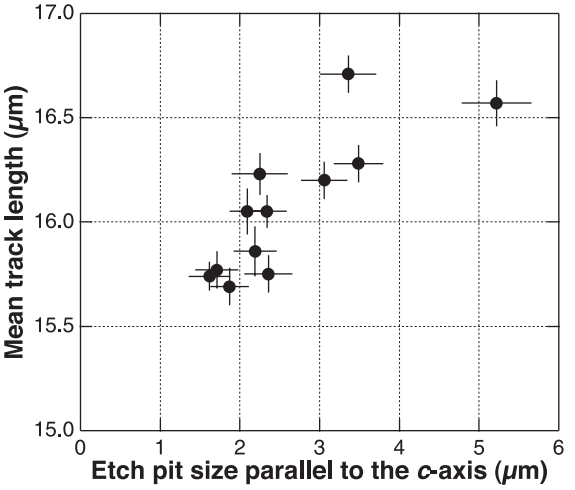


Fig. 8. Variation of unannealed induced confined track length vs. size of etch pit parallel to the *c*-axis (dpar of Donelick, 1993; Burtner et al., 1994; Carlson et al., 1999) for apatite samples of differing composition. Samples etched 5 M $HNO_3$, 20 ± 1 °C, 20 s; TINTs only measured; ~ 100 tracks per measurement; single analyst. Lengths measured using transmitted light, etch pits reflected light microscopy. Error bars ± 1 standard error.

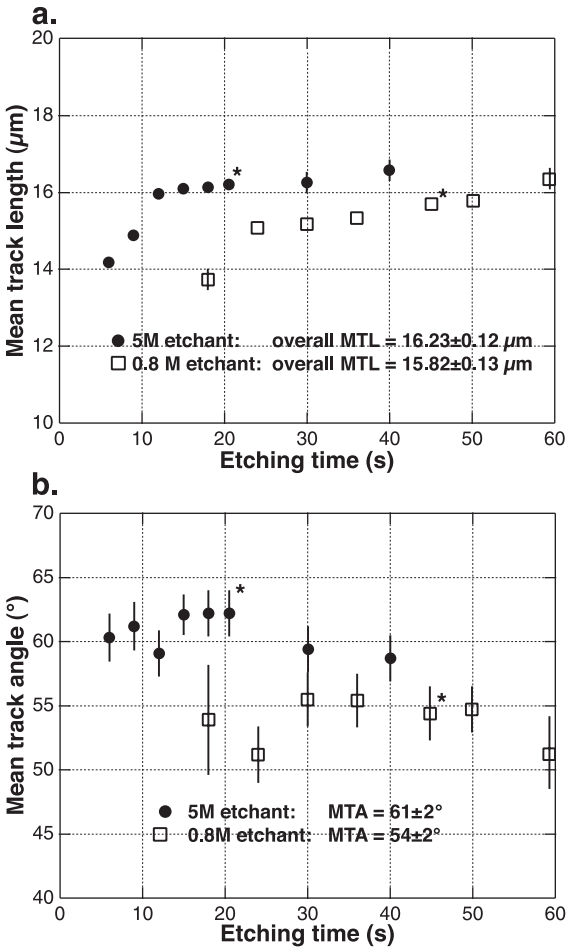


Fig. 9. Lengths and angles measured in FCT apatite in step-etching experiments using 5 M and 0.8 M $HNO_3$ etchants. Starred points show commonly used etch times. Unannealed induced tracks. Both TINTs and TINCLEs measured by one analyst. Errors on individual points are ± 1 standard error and lie mostly within the plotted symbols. Errors on overall means are also ± 1 standard error.

axis are thin while tracks perpendicular to it are fatter. The size and shape of an etched track are also a function of apatite chemistry (Gleadow, 1981; Laslett et al., 1984), with chlorine-rich apatites having larger tracks and etch pits when compared to fluorine-rich apatites (e.g. Burtner et al., 1994; Carlson et al., 1999). Fig. 8 shows a clear relationship between MTL and etch pit size for unannealed induced (i.e. full-length) tracks for apatites of varying composition etched identically. Donelick (1993) has advocated the use of etch pit size as a measure for estimating apatite composition.

Most FT laboratories favour as apatite etchant either 5 M $HNO_3$ for 20 s, or 0.8 M $HNO_3$ for 45 s, each at room temperature. Since it is generally assumed that a fully-exposed track length is obtained after a certain etch time specific to the acid concentration and temperature, the question arises whether these two most commonly used etchants give comparable results. Optimum etch times may be defined by step-etch experiments (Laslett et al., 1984; Watt and Durrani, 1985; Crowley et al., 1991). Fig. 9a compares the results from such a step-etching experiment for the simplest case of a unimodal distribution of long tracks. Induced tracks in two aliquots of Fish Canyon Tuff apatite were step etched using 5 M

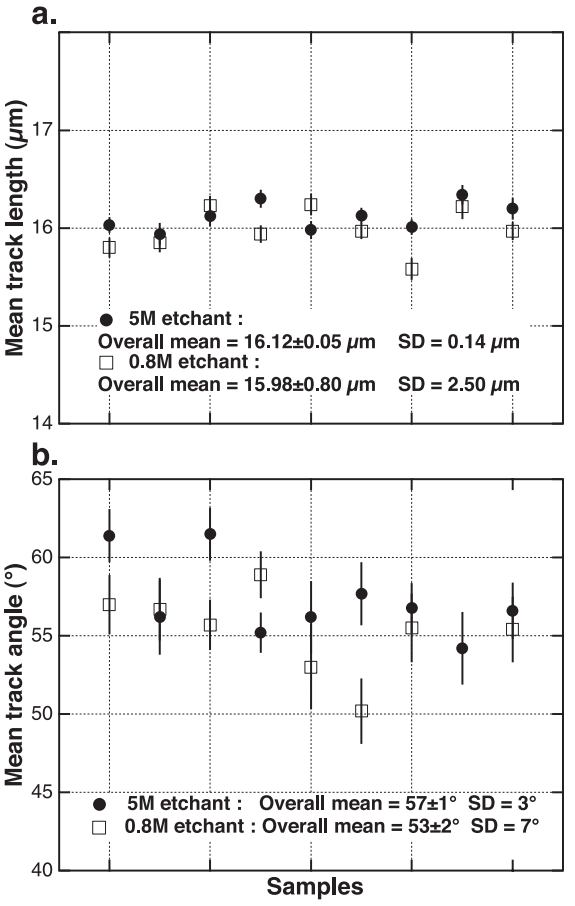


Fig. 10. Comparison of MTL and MTA values resulting from 0.8 M and 5 M $HNO_3$ etching of separate aliquots of apatites of varying composition. Samples contained induced tracks. TINTs only measured; 100 tracks for each analysis. ± 1 S.E.M. One analyst.

$HNO_3$ and 0.8 M $HNO_3$ each at 20 ± 1 °C up to etch times used routinely for samples (viz. 20 and 45 s, respectively) and beyond. The results from each etchant define an approximate plateau, the weaker etchant more slowly with a shorter final track length at the commonly used 45-s etch time. The 5 and 0.8 M MTL values from the etch steps at the commonly used times (20 and 45 s, respectively) differ by ~ 0.4 μm, although they overlap within 95% confidence limits. With prolonged etching to 60 s, the MTL for the weaker etchant is indistinguishable from that of the stronger etchant at shorter etch times. The MTAs revealed by each etchant (Fig. 9b) show slight variations between etch steps, but for each acid, individual values lie within analytical uncertainties. The weak 0.8 M acid gives an MTA = 54 ± 2°, nearer to the ideal MTA value of 45° for randomly orientated tracks. The 5 M etchant gives an MTA of 61 ± 2° with fewer tracks at low angles to the *c*-axis, indicating greater etching anisotropy.

Comparative etching of unannealed, induced tracks in nine further samples of varying composition revealed a trend toward longer MTLs for most, but not all, of those aliquots etched with the 5 M acid (see

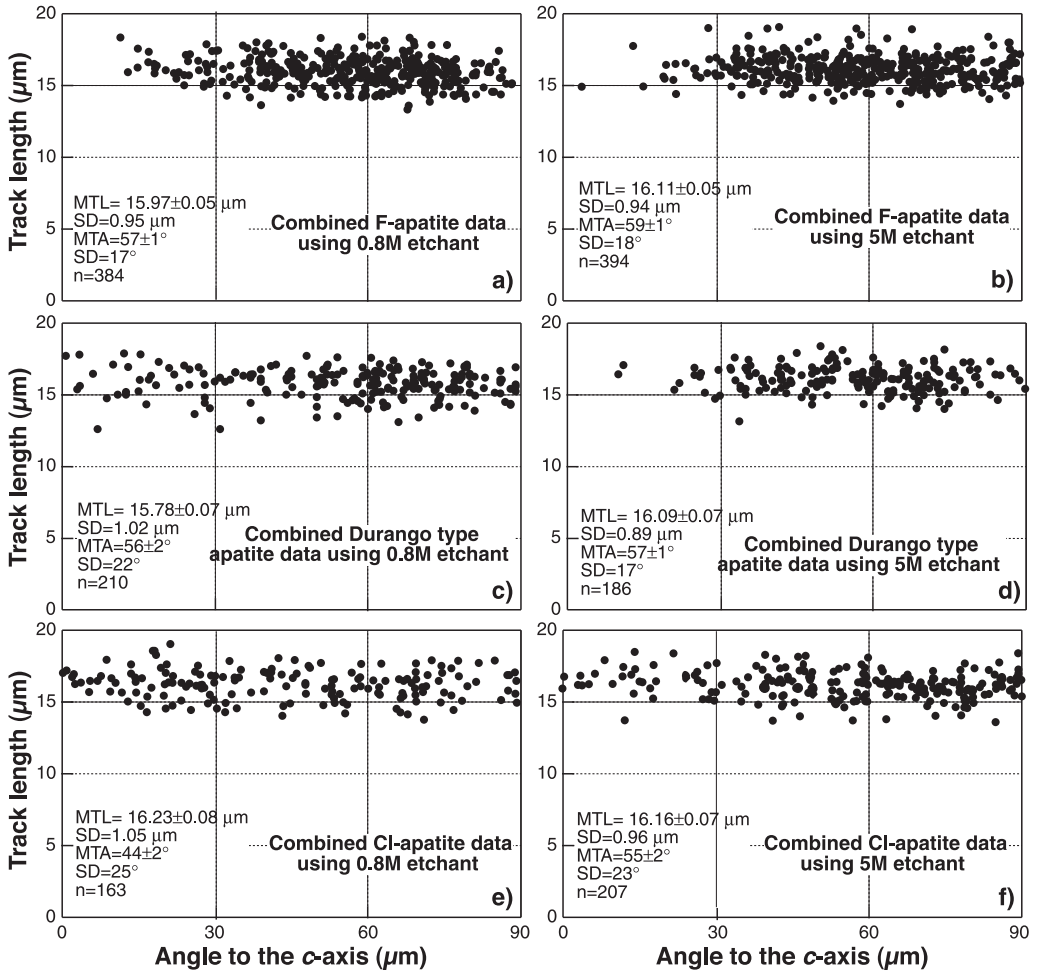


Fig. 11. Comparison of angular distribution of unannealed induced tracks (all TINTs) revealed in separate sample aliquots using 0.8 and 5 M $HNO_3$. a and b compare data combined from five large fluor-apatites (Cl < 0.01 apfu). c and d compare data combined from two apatite samples with Cl ± 0.12 apfu and e and f from three large chlor-apatites (Cl>0.25 apfu).

Table 3
TINT and TINCLE measurements by a single analyst on the same apatite mounts of 74 samples

| Sample | TINTS | | | | | TINCLES | | | | |
|---|---|---|---|---|---|---|---|---|---|---|
| | MTL (μm) ± 1 S.E.M. | ± 1 S.D. | *N* | MTA (°) ± 1 S.E.M. | ± 1 S.D. | MTL (μm) ± 1 S.E.M. | ± 1 S.D. | *N* | MTA (°) ± 1 S.E.M. | ± 1 S.D. |
| BAM-Un* | 16.57 ± 0.11 | 1.06 | 100 | 51 ± 2 | 22 | 16.32 ± 0.15 | 1.10 | 52 | 61 ± 3 | 21 |
| GIL-Un* | 16.23 ± 0.10 | 0.95 | 100 | 61 ± 2 | 22 | 16.32 ± 0.08 | 0.78 | 101 | 72 ± 1 | 15 |
| MIN-Un* | 16.20 ± 0.09 | 0.90 | 100 | 57 ± 2 | 18 | 16.40 ± 0.12 | 0.91 | 64 | 50 ± 3 | 21 |
| DRV-Un* | 16.05 ± 0.08 | 0.80 | 100 | 59 ± 2 | 18 | 15.68 ± 0.16 | 1.04 | 41 | 57 ± 3 | 20 |
| FUL-Un* | 16.05 ± 0.11 | 0.79 | 55 | 54 ± 3 | 22 | 16.18 ± 0.10 | 0.76 | 61 | 57 ± 3 | 26 |
| UMB-Un* | 15.86 ± 0.12 | 0.76 | 41 | 58 ± 3 | 21 | 16.06 ± 0.12 | 0.91 | 62 | 65 ± 2 | 18 |
| DUR-Un* | 15.77 ± 0.09 | 0.86 | 100 | 54 ± 2 | 17 | 16.08 ± 0.07 | 0.73 | 100 | 63 ± 2 | 15 |
| WIL-Un* | 15.74 ± 0.07 | 0.71 | 100 | 58 ± 2 | 16 | 15.84 ± 0.09 | 0.91 | 101 | 61 ± 2 | 17 |
| UNK-Un* | 15.69 ± 0.09 | 0.88 | 100 | 57 ± 2 | 22 | 16.15 ± 0.09 | 0.86 | 100 | 56 ± 2 | 19 |
| BAM200B | 15.40 ± 0.09 | 0.92 | 100 | 55 ± 2 | 22 | 15.33 ± 0.21 | 1.33 | 43 | 54 ± 3 | 22 |
| MIN200B | 15.10 ± 0.10 | 0.95 | 100 | 57 ± 2 | 24 | 15.30 ± 0.24 | 1.18 | 24 | 61 ± 4 | 21 |
| FUL200B | 15.02 ± 0.08 | 0.81 | 100 | 57 ± 2 | 21 | 15.47 ± 0.12 | 0.98 | 68 | 56 ± 3 | 21 |
| BAM240B | 14.98 ± 0.09 | 0.85 | 100 | 53 ± 2 | 22 | 15.43 ± 0.34 | 1.69 | 25 | 53 ± 5 | 26 |
| GIL200B | 14.98 ± 0.09 | 0.89 | 100 | 57 ± 2 | 23 | 15.37 ± 0.15 | 1.03 | 47 | 71 ± 2 | 16 |
| UMB200B | 14.85 ± 0.08 | 0.75 | 100 | 61 ± 2 | 21 | 15.06 ± 0.10 | 1.00 | 100 | 61 ± 2 | 23 |
| UNK200B | 14.74 ± 0.07 | 0.74 | 100 | 57 ± 2 | 20 | 15.09 ± 0.12 | 1.20 | 100 | 61 ± 2 | 19 |
| DUR200B | 14.66 ± 0.08 | 0.77 | 100 | 57 ± 2 | 23 | 15.02 ± 0.11 | 1.05 | 100 | 64 ± 2 | 18 |
| WIL200B | 14.63 ± 0.09 | 0.90 | 100 | 57 ± 2 | 18 | 14.90 ± 0.08 | 0.77 | 106 | 64 ± 2 | 16 |
| DRV200B | 14.50 ± 0.08 | 0.80 | 100 | 62 ± 2 | 19 | 14.85 ± 0.19 | 0.99 | 27 | 55 ± 4 | 20 |
| MIN240B | 14.22 ± 0.09 | 0.90 | 100 | 60 ± 2 | 20 | 14.42 ± 0.16 | 1.20 | 55 | 63 ± 2 | 18 |
| UMB240B | 14.19 ± 0.07 | 0.71 | 100 | 57 ± 2 | 20 | 14.37 ± 0.10 | 0.95 | 84 | 68 ± 2 | 15 |
| DUR240B | 14.07 ± 0.09 | 0.85 | 100 | 61 ± 2 | 17 | 14.04 ± 0.09 | 0.90 | 100 | 63 ± 2 | 16 |
| GIL240B | 14.02 ± 0.09 | 0.86 | 100 | 61 ± 2 | 22 | 14.43 ± 0.14 | 1.00 | 55 | 69 ± 3 | 20 |
| FUL280B | 13.86 ± 0.09 | 0.93 | 100 | 55 ± 2 | 19 | 13.84 ± 0.10 | 1.02 | 100 | 68 ± 2 | 16 |
| BAM275B | 13.83 ± 0.10 | 0.99 | 100 | 55 ± 2 | 23 | 14.44 ± 0.26 | 1.42 | 30 | 59 ± 4 | 24 |
| BAM280B | 13.81 ± 0.09 | 0.90 | 100 | 54 ± 2 | 22 | 14.03 ± 0.14 | 1.31 | 87 | 53 ± 2 | 22 |
| DRV240B | 13.72 ± 0.07 | 0.71 | 101 | 61 ± 2 | 18 | 13.77 ± 0.20 | 1.12 | 32 | 58 ± 3 | 17 |
| UNK240B | 13.48 ± 0.08 | 0.78 | 100 | 57 ± 2 | 23 | 13.84 ± 0.10 | 0.95 | 100 | 58 ± 2 | 19 |
| FUL275B | 13.36 ± 0.08 | 0.84 | 100 | 60 ± 2 | 23 | 13.54 ± 0.10 | 0.97 | 100 | 62 ± 2 | 18 |
| WIL240B | 13.34 ± 0.08 | 0.75 | 100 | 61 ± 2 | 16 | 13.88 ± 0.09 | 0.88 | 100 | 64 ± 2 | 15 |
| UMB280B | 13.18 ± 0.10 | 1.01 | 100 | 54 ± 2 | 20 | 13.07 ± 0.13 | 1.27 | 101 | 64 ± 2 | 19 |
| UMB275B | 13.11 ± 0.10 | 1.03 | 101 | 58 ± 2 | 20 | 13.46 ± 0.09 | 0.94 | 100 | 63 ± 2 | 18 |
| BAM300B | 13.03 ± 0.11 | 1.06 | 100 | 52 ± 2 | 21 | 13.61 ± 0.28 | 1.50 | 30 | 60 ± 4 | 24 |
| MIN280B | 12.88 ± 0.10 | 1.03 | 100 | 59 ± 2 | 23 | 13.20 ± 0.10 | 0.97 | 100 | 57 ± 2 | 19 |
| MIN275B | 12.80 ± 0.10 | 1.02 | 100 | 59 ± 2 | 19 | 12.90 ± 0.10 | 0.97 | 92 | 68 ± 2 | 17 |
| DUR280B | 12.71 ± 0.11 | 1.05 | 100 | 57 ± 2 | 18 | 12.79 ± 0.08 | 0.83 | 100 | 65 ± 2 | 16 |
| DUR275B | 12.64 ± 0.08 | 0.79 | 100 | 63 ± 2 | 19 | 12.78 ± 0.13 | 0.95 | 58 | 66 ± 2 | 15 |
| FUL300B | 12.55 ± 0.09 | 0.85 | 100 | 55 ± 2 | 21 | 12.36 ± 0.09 | 0.92 | 100 | 65 ± 2 | 19 |
| GIL275B | 12.44 ± 0.10 | 0.97 | 100 | 62 ± 2 | 21 | 12.61 ± 0.13 | 0.94 | 52 | 65 ± 2 | 17 |
| GUN335B | 12.18 ± 0.09 | 0.86 | 100 | 55 ± 2 | 20 | 11.33 ± 0.13 | 1.29 | 100 | 61 ± 2 | 23 |
| WIL275B | 12.17 ± 0.09 | 0.85 | 100 | 58 ± 2 | 22 | 12.34 ± 0.13 | 1.06 | 71 | 59 ± 3 | 23 |
| GIL280B | 12.06 ± 0.10 | 1.00 | 100 | 56 ± 2 | 22 | 12.50 ± 0.10 | 0.95 | 100 | 66 ± 2 | 16 |
| UNK275B | 11.96 ± 0.09 | 0.90 | 100 | 57 ± 2 | 17 | 12.18 ± 0.13 | 1.30 | 100 | 59 ± 2 | 18 |
| BAM312B | 11.91 ± 0.12 | 1.22 | 101 | 53 ± 2 | 21 | 12.64 ± 0.12 | 1.17 | 90 | 49 ± 3 | 26 |
| MIN300B | 11.81 ± 0.10 | 0.96 | 100 | 61 ± 2 | 19 | 12.30 ± 0.11 | 1.13 | 100 | 56 ± 2 | 23 |
| BAM320B | 11.67 ± 0.13 | 1.34 | 100 | 47 ± 2 | 24 | 11.47 ± 0.31 | 1.71 | 32 | 61 ± 5 | 26 |
| WIL280B | 11.67 ± 0.09 | 0.90 | 100 | 61 ± 2 | 18 | 11.99 ± 0.12 | 1.15 | 100 | 62 ± 2 | 18 |
| UMB300B | 11.59 ± 0.13 | 1.15 | 82 | 60 ± 2 | 21 | 11.78 ± 0.28 | 1.88 | 46 | 67 ± 3 | 20 |
| DRV280B | 11.43 ± 0.11 | 1.11 | 100 | 61 ± 2 | 16 | 12.09 ± 0.10 | 1.01 | 100 | 62 ± 2 | 16 |
| UNK280B | 11.34 ± 0.10 | 1.02 | 100 | 60 ± 2 | 20 | 11.83 ± 0.12 | 1.23 | 100 | 60 ± 2 | 20 |
| BAM325B | 11.18 ± 0.14 | 1.35 | 100 | 58 ± 2 | 24 | 11.69 ± 0.43 | 1.98 | 22 | 59 ± 5 | 23 |

Table 3 (*continued*)

| Sample | TINTS | | | | | TINCLES | | | | |
|---|---|---|---|---|---|---|---|---|---|---|
| | MTL (μm) ± 1 S.E.M. | ± 1 S.D. | *N* | MTA (°) ± 1 S.E.M. | ± 1 S.D. | MTL (μm) ± 1 S.E.M. | ± 1 S.D. | *N* | MTA (°) ± 1 S.E.M. | ± 1 S.D. |
| DUR300B | 11.18 ± 0.11 | 1.05 | 100 | 56 ± 2 | 23 | 11.15 ± 0.12 | 1.17 | 100 | 58 ± 2 | 23 |
| FUL320B | 11.03 ± 0.11 | 1.11 | 100 | 57 ± 2 | 20 | 11.36 ± 0.12 | 0.92 | 58 | 49 ± 3 | 22 |
| FUL312B | 10.69 ± 0.26 | 1.52 | 34 | 47 ± 4 | 26 | 11.56 ± 0.20 | 1.24 | 39 | 58 ± 3 | 20 |
| DUR312B | 10.24 ± 0.14 | 1.37 | 102 | 56 ± 2 | 18 | 10.6 ± 0.10 | 1.05 | 104 | 62 ± 1 | 15 |
| UMB312B | 10.09 ± 0.14 | 1.39 | 101 | 61 ± 2 | 21 | 10.36 ± 0.13 | 1.34 | 100 | 65 ± 2 | 17 |
| UMB320B | 9.92 ± 0.18 | 1.60 | 80 | 50 ± 3 | 24 | 11.32 ± 0.32 | 1.93 | 37 | 58 ± 3 | 17 |
| DRV300B | 9.91 ± 0.14 | 1.37 | 100 | 54 ± 2 | 17 | 9.94 ± 0.14 | 1.35 | 100 | 56 ± 2 | 21 |
| MIN312B | 9.89 ± 0.18 | 1.82 | 100 | 58 ± 2 | 18 | 10.11 ± 0.18 | 1.82 | 100 | 61 ± 2 | 19 |
| GIL300B | 9.61 ± 0.18 | 1.78 | 100 | 56 ± 2 | 22 | 9.60 ± 0.13 | 1.29 | 100 | 64 ± 2 | 18 |
| WIL300B | 9.33 ± 0.22 | 2.18 | 100 | 54 ± 2 | 19 | 9.95 ± 0.15 | 1.49 | 100 | 60 ± 2 | 18 |
| UNK300B | 9.17 ± 0.23 | 2.14 | 88 | 52 ± 2 | 23 | 10.60 ± 0.19 | 1.90 | 100 | 53 ± 2 | 20 |
| DUR320B | 8.70 ± 0.23 | 2.30 | 100 | 53 ± 2 | 20 | 9.19 ± 0.25 | 2.40 | 91 | 56 ± 3 | 24 |
| UMB325B | 8.70 ± 0.21 | 2.14 | 100 | 49 ± 2 | 18 | 10.20 ± 0.30 | 2.45 | 68 | 58 ± 3 | 22 |
| DUR325B | 8.69 ± 0.24 | 2.40 | 100 | 46 ± 2 | 24 | 9.50 ± 0.30 | 2.12 | 50 | 37 ± 3 | 21 |
| MIN325B | 8.44 ± 0.22 | 2.23 | 100 | 46 ± 2 | 20 | 10.13 ± 0.17 | 1.59 | 94 | 35 ± 2 | 20 |
| MIN320B | 8.10 ± 0.25 | 2.49 | 100 | 51 ± 2 | 21 | 10.04 ± 0.31 | 2.56 | 68 | 47 ± 3 | 24 |
| DRV287C | 7.59 ± 0.37 | 2.73 | 55 | 33 ± 2 | 15 | 11.02 ± 0.21 | 2.04 | 100 | 45 ± 3 | 25 |
| GIL312B | 7.51 ± 0.26 | 2.62 | 100 | 31 ± 2 | 21 | 8.19 ± 0.60 | 2.16 | 14 | 42 ± 6 | 23 |
| DRV320B | 7.36 ± 0.23 | 2.27 | 100 | 24 ± 2 | 14 | 11.13 ± 0.31 | 2.26 | 55 | 41 ± 4 | 30 |
| WL312B | 6.59 ± 0.30 | 3.00 | 100 | 49 ± 2 | 23 | 8.81 ± 0.31 | 3.06 | 100 | 40 ± 2 | 22 |
| DRV312B | 6.50 ± 0.28 | 2.79 | 100 | 42 ± 2 | 16 | 11.78 ± 0.26 | 2.59 | 100 | 45 ± 2 | 23 |
| DRV325B | 6.39 ± 0.22 | 2.23 | 100 | 21 ± 2 | 16 | 10.09 ± 0.40 | 2.30 | 34 | 33 ± 5 | 26 |
| UNK312B | 6.17 ± 0.30 | 3.03 | 100 | 38 ± 2 | 22 | 12.08 ± 0.29 | 2.59 | 80 | 59 ± 2 | 18 |

Samples contain induced tracks; * are unannealed; remainder are partially annealed during laboratory experiments; see Barbarand et al., submitted for publication. Samples etched 5 M $HNO_3$ 20 ± 1 °C 20 s.

Fig. 10a). Smaller MTAs were found for samples etched with the weaker 0.8 M acid, although one apatite gave a larger MTA (0.8 M: 59 ± 2° vs. 5 M: 55 ± 1°)—see Fig. 10b. In nearly all cases, 0.8 vs. 5 M variation exceeds the differences found between replicate analysis by a single observer for same apatites but using a single etchant (see Table 1).

The relationship between angle, etchant and apatite composition can be revealed further if the same data are plotted with individual track lengths shown relative to their angle to the *c*-axis: in Fig. 11, data are grouped according to Cl content of the host apatite. In Fig. 11a and b, fluor-apatites (Cl < 0.01 apfu or < 0.01 wt.%) show the MTLs for the 0.8 and 5 M etched samples to overlap within two standard errors. The MTA for 5 M is slightly greater than that for 0.8 M, shown also by the relative paucity of tracks at low angles to the *c*-axis in the aliquot treated by the stronger etchant. For Durango and other data where Cl is 0.12 apfu ( ~ 0.4 wt.%), the plot shows a clear difference in the angular distribution of the tracks (Fig. 11c and d) for the two etchants, with a more uniform spread for the weaker acid. MTA values overlap within two standard errors again emphasising this to be a relatively insensitive measure of variation. The combined data from three large chlor-apatites (Cl>0.25 apfu or >0.5 wt.%) show very similar MTL values within one standard error for the two etchants (Fig. 11 e and f). There is also an apparent similarity in the angular distribution of tracks with a significant proportion of low-angle tracks present in the 5 M etched aliquots. Etching anisotropy when using the 5 M etchant is reduced for chlor-apatites, the general etch rates in different directions being similar, resulting in larger, broader etch pits (see Fig. 8). Nevertheless, MTAs still differ substantially between the two etchants, $MTA_{0.8\ M}$ at 44 ± 2° being indistinguishable from the theoretical value of 45° and showing the most isotropic distribution in the study (Fig. 11e). The higher $MTA_{5\ M}$ of 55 ± 2° can be seen to result from a much higher cohort of tracks at highest angles to the *c*-axis.

The probability of observing and measuring a fission track depends on the shape and size of the etch pit, factors controlled by *c*-axis orientation, apatite composition and etchant. The question thus arises as to which etchant is better used to generate FT data for geological applications? Observational bias models could be constructed for either etchant provided a consistent experimental approach is adopted. For full-length tracks, the above experiments show that choice of etchant has a marginal effect on MTL, but that 5 M $HNO_3$ produces significantly more angular anisotropy, especially with fluor-apatite, the most abundant apatite species in upper crustal samples. In principle, therefore, the more isotropic etching nature of the weaker acid, producing an MTA closer to the theoretical value, seems to favour 0.8 M $HNO_3$ as etchant. However, after extensive comparisons, two practical reasons persuade us to favour use of the stronger 5 M $HNO_3$ etchant. Firstly, tracks revealed by the weaker 0.8 M acid are thin, with poorly defined track ends, making measurement speculative. In contrast, the stronger 5 M etchant produces broader tracks, with well-defined, unambiguous track ends, critical for robust analysis of track length. Such tracks are easier to see and can be measured with confidence. Secondly, the 5 M etchant produces well-defined etch pits: aligned etch pits, best viewed under incident illumination, are diagnostic of prismatic, *c*-axis parallel sections of apatite. Such prismatic sections provide a uniform etching response, with a high efficiency and low bulk etch rate, permitting robust evaluation of the geometry factor necessary for use with the external detector method. This alignment of etch pits is not readily discernible with the 0.8 M acid leading to selection and analysis of randomly oriented apatite sections with variable bulk etch rates and undefined geometry.

For these practical reasons, all further data in this and the companion annealing studies have been generated by etching apatite with 5 M $HNO_3$ at 20 ± 1 °C for 20 s.

### 6.2. TINTs and TINCLEs

Horizontal confined track lengths are revealed by etchant passing through either surface tracks to give Track-IN-Track (TINTs) or through cleavage planes or cracks to give Track-IN-Cleavage (TINCLEs) (Lal et al., 1969; Bhandari et al., 1971; Laslett et al., 1982). Measurement of each type of track has its own bias. The value and reliability of TINCLE measurements has often been debated (e.g. Laslett et al., 1984; Carlson et al., 1999), but no published study has established whether the information provided by TINTs and TINCLEs is equivalent. Galbraith et al. (1990) have reported that for a given sample, TINCLE measurements tend to be longer than TINTs.

We have compared TINT and TINCLE measurements on 74 aliquots of apatite of varying composition and different levels of annealing to test a broad range of track shapes and length distributions (Table 3). Fig. 12 plots $MTL_{TINT}$ against $MTL_{TINCLE}$ for the same samples and shows varying levels of deviation from a 1:1 relationship. For track populations with MTLs>15 μm, the data spread close to the line indicating similarity of TINT and TINCLE values. Between 15 and 12 μm, TINCLEs are systematically slightly longer than TINTs. For more heavily annealed samples with MTL values <12 μm, the differences become much wider with TINCLEs substantially longer than TINTs. Plotting individual track length vs. angle to the *c*-axis for samples with moderate to high levels of track annealing shows that, in contrast to TINTs, there are relatively few short TINCLEs at high angles. Long TINCLEs dominate almost irrespective of angle (Fig. 13). This indicates that in these moderately annealed samples, measurement of TINCLEs masks the anisotropy of annealing.

Several sources have been proposed for bias in TINCLE measurement (Laslett et al., 1982; Galbraith et al., 1990) and these apply to the data generated in this study:

- A cleavage-induced preferred orientation: a TINCLE is more likely to intersect a fracture if its angle to the fracture is higher (nearer 90° rather than nearer 0°); the angular distribution will depart from a uniform one if host fractures run in a preferred direction.
- Exclusion of short tracks: short tracks may be hidden within wider fractures as the probability of a track crossing a fracture is directly proportional to its length (Green, 1988).
- Movement of fractures: during polishing or sample preparation, the cleavage or fracture may be widened before etching.

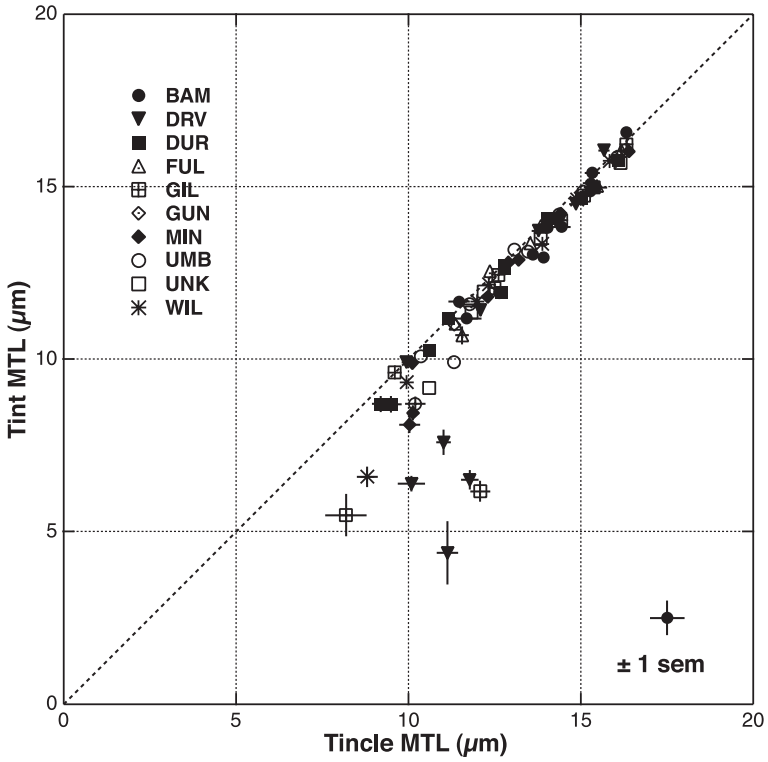


Fig. 12. Relationship between TINT and TINCLE mean track lengths measured on the same apatite samples of differing compositions, induced tracks annealed at various levels in laboratory experiments. Samples etched 5 M $HNO_3$, 20 ± 1 °C, 20 s; single analyst on same apatite mounts; ~ 100 tracks per measurement. Error bars ± 1 standard error, for most samples lying within plotted points.

- Increased etch rates along fractures: tracks in fractures are etched more readily because etchant can access the confined track more easily through wider or larger channels. Jonckheere and Wagner (2000) have suggested that the action of fluids circulating over geological time could act as natural etching for such tracks, thus promoting the longer length of TINCLEs.

The use of fractures to observe confined tracks substantially excludes the measurement of short tracks and therefore modifies significantly the MTL of heavily annealed samples. Random measurement of both TINTs and TINCLEs will give a significant bias toward longer lengths, a bias difficult to quantify as it will vary according to the TINT/TINCLE ratio measured and to the level of annealing in the sample. In this study, the difference between TINT and TINCLE has been exaggerated by their separate analysis; a conventional analysis would comprise TINTs *and* TINCLEs. As mean track lengths below 12 μm are less common for geological samples at outcrop, the bias involved in measuring TINCLEs is relatively small and a case for analysis using both TINTs and TINCLEs might be argued—although we suggest that the TINCLE bias should be avoided completely. For borehole samples where annealing levels may be greater, or in annealing calibration experiments where MTLs are < 12 μm, the bias to longer lengths introduced by measuring TINCLEs is difficult to quantify and is not ideal. The Laslett et al. (1987) annealing algorithm utilised the Green et al. (1986) annealing data measured using both TINTs and TINCLEs on the Durango apatite, and is thus subject to the TINCLE bias, a point to be considered by anyone using the algorithm.

Our experiments confirm the views of Laslett et al. (1982), Galbraith et al. (1990) and Carlson et al. (1999) that in practice only TINT confined tracks

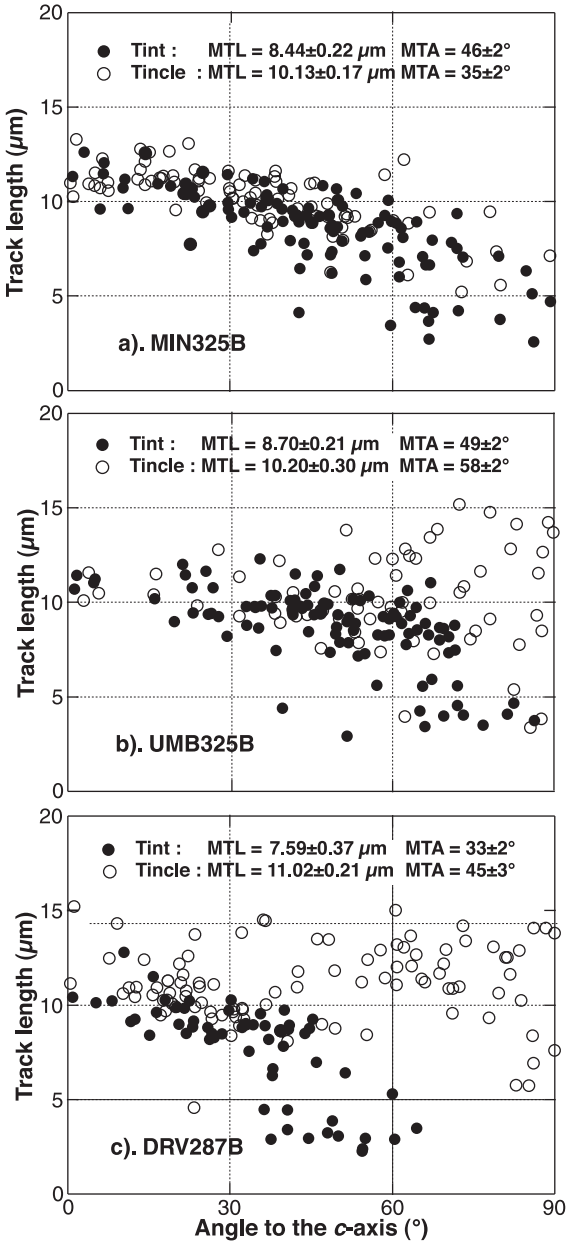


Fig. 13. Track length vs. angle to the *c*-axis for TINT and TINCLE measurements for three partially annealed apatite samples in Fig. 12. Uncertainties are ± 1 standard error.

should be measured. Despite the resulting restriction this places on sampling, we believe that TINCLEs should be excluded from track-length measurement.

### 6.3. Use of $^{252}$Cf-derived fission fragments

By restricting measurement of confined track-length to TINTs because of the unknown bias introduced by sampling TINCLEs, the number of tracks available for length analysis is substantially reduced. This sampling problem may be exacerbated in very young or highly annealed samples, where track numbers are small and the probability of intersecting a shortened, confined track is greatly reduced. Various suggestions have been proffered to increase the chance of finding additional tracks by introducing artificial etching conduits to facilitate passage of acid to the confined track (Yamada et al., 1998). Mechanical fracturing results in production of further TINCLEs and can be dismissed. In contrast, irradiation with a collimated beam of heavy ions such as $^{252}$Cf-derived fission fragments (Donelick and Miller, 1991) will result in additional TINTs, boosting the track-length sample and, hopefully, improving analytical precision. However, heavy ion irradiation may introduce an additional observational bias.

To evaluate this potentially highly useful aid to analysis, we compared track lengths and angles in natural and Cf-irradiated aliquots of 25 apatites of differing composition and of varying levels of partial annealing to ensure assessment of a wide range of MTLs and track-length distributions. For each sample, track lengths and angles were first measured, the samples repolished and then irradiated with $^{252}$Cf fission fragments, re-etched and lengths and angles measured a second time. A 37-kBq Cf source was used in vacuo; a collimated beam of tracks at high angle to the sample surface was achieved by maintaining a space of ~ 20 mm between source and sample to ensure that low-angle tracks ranged out. An exposure time of 24 h produced a $^{252}$Cf fission-track density of ~ $10^5$ per cm$^2$. The same analyst made all measurements.

Track length and angle results are given in Table 4 and a 1:1 plot of MTL with and without Cf irradiation shown in Fig. 14. Overall deviation between the two datasets is about 3%, similar to that found for replicate analysis by a single analyst (cf. Fig. 3). In samples where the MTL is long, there is no significant difference between the two datasets. For samples where MTL < ~ 14 μm, there is a slight systematic shift to longer values for the Cf-irradiated samples, with 3 of the 25 samples deviating by more than two standard

Table 4
Length and angle measurement of the same mounts with and without the use of $^{252}$Cf-derived fission fragments

| Sample | Without Cf-derived fission fragment | | | | | With Cf-derived fission fragment | | | | |
|---|---|---|---|---|---|---|---|---|---|---|
| | MTL (μm) ± 1 S.E.M. | ± 1 S.D. | *N* | MTA (°) ± 1 S.E.M. | ± 1 S.D. | MTL (μm) ± 1 S.E.M. | ± 1 S.D. | *N* | MTA (°) ± 1 S.E.M. | ± 1 S.D. |
| DUR200B | 14.98 ± 0.08 | 0.80 | 101 | 56 ± 1 | 15 | 14.89 ± 0.07 | 0.73 | 102 | 59 ± 2 | 18 |
| BAM240B | 14.92 ± 0.09 | 0.85 | 101 | 54 ± 2 | 21 | 14.94 ± 0.09 | 0.89 | 104 | 51 ± 2 | 24 |
| WIL200B | 14.75 ± 0.07 | 0.70 | 101 | 62 ± 1 | 14 | 14.84 ± 0.07 | 0.73 | 101 | 59 ± 2 | 16 |
| GUN280B | 14.36 ± 0.08 | 0.77 | 101 | 55 ± 2 | 20 | 14.34 ± 0.09 | 0.90 | 103 | 55 ± 2 | 20 |
| UMB240B | 14.27 ± 0.08 | 0.81 | 103 | 57 ± 2 | 20 | 14.38 ± 0.08 | 0.77 | 101 | 60 ± 2 | 20 |
| DUR240B | 14.16 ± 0.07 | 0.69 | 101 | 57 ± 2 | 16 | 14.13 ± 0.07 | 0.67 | 100 | 59 ± 2 | 15 |
| UMB270A | 14.07 ± 0.08 | 0.77 | 103 | 62 ± 2 | 20 | 14.22 ± 0.08 | 0.84 | 101 | 64 ± 2 | 19 |
| DUR270A | 14.07 ± 0.07 | 0.66 | 101 | 56 ± 2 | 19 | 14.06 ± 0.06 | 0.63 | 101 | 60 ± 2 | 16 |
| GIL240B | 14.03 ± 0.07 | 0.74 | 102 | 52 ± 2 | 23 | 13.96 ± 0.08 | 0.78 | 99 | 57 ± 2 | 20 |
| FUL275B | 13.30 ± 0.06 | 0.65 | 101 | 59 ± 1 | 15 | 13.65 ± 0.07 | 0.69 | 102 | 59 ± 2 | 16 |
| FUL300B | 12.67 ± 0.08 | 0.83 | 102 | 55 ± 2 | 18 | 12.77 ± 0.08 | 0.76 | 102 | 56 ± 2 | 18 |
| DRV275B | 12.57 ± 0.08 | 0.83 | 102 | 57 ± 2 | 17 | 12.72 ± 0.07 | 0.75 | 101 | 56 ± 2 | 17 |
| FAR280B | 11.78 ± 0.09 | 0.90 | 101 | 53 ± 2 | 22 | 11.76 ± 0.08 | 0.84 | 100 | 56 ± 2 | 17 |
| WIL280B | 11.66 ± 0.08 | 0.81 | 102 | 57 ± 1 | 14 | 11.88 ± 0.08 | 0.78 | 102 | 58 ± 1 | 15 |
| DUR300B | 11.09 ± 0.07 | 0.74 | 102 | 60 ± 2 | 17 | 11.20 ± 0.08 | 0.80 | 102 | 59 ± 2 | 18 |
| DUR325B | 9.24 ± 0.19 | 1.90 | 102 | 44 ± 2 | 19 | 8.14 ± 0.28 | 2.84 | 103 | 50 ± 2 | 20 |
| MIN325B | 8.81 ± 0.23 | 2.35 | 100 | 42 ± 2 | 21 | 9.08 ± 0.22 | 2.17 | 102 | 42 ± 2 | 18 |
| MIN320B | 8.57 ± 0.23 | 2.31 | 100 | 47 ± 2 | 20 | 9.25 ± 0.20 | 2.04 | 102 | 44 ± 2 | 16 |
| UMB325B | 8.39 ± 0.25 | 2.51 | 100 | 49 ± 2 | 21 | 8.71 ± 0.21 | 2.08 | 103 | 51 ± 2 | 20 |
| GUN360B | 8.20 ± 0.23 | 2.44 | 109 | 48 ± 2 | 23 | 9.01 ± 0.23 | 2.31 | 102 | 41 ± 2 | 22 |
| DRV325B | 6.81 ± 0.22 | 2.20 | 101 | 20 ± 1 | 13 | 7.23 ± 0.21 | 2.08 | 100 | 18 ± 1 | 11 |
| WIL312B | 5.37 ± 0.30 | 2.97 | 100 | 46 ± 2 | 24 | 5.83 ± 0.54 | 3.48 | 43 | 49 ± 3 | 21 |

Samples contain induced tracks, partially annealed during laboratory experiments; see Barbarand et al., submitted for publication. Samples were repolished and re-etched after $^{252}$Cf irradiation; exposure time 24 h. Samples etched for 5 M $HNO_3$ 20 ± 1 °C 20 s. TINTs only measured by a single analyst.

errors from the 1:1 plot. A single sample shows a reverse trend with the Cf-irradiated aliquot producing a shorter MTL, significant at two standard errors. No systematic trend is found for MTA values in samples with and without Cf-irradiation, the mean difference between values of ~ 5% being only slightly larger than that found for replicate analysis by a single analyst (Table 1). Fig. 15 shows length vs. angle plots for two contrasting samples, which illustrate situations where enhanced track numbers would be beneficial. In Fig. 15a, all tracks are long as would be found in a rapidly exhumed, youthful orogen such as the Himalayas. Fig. 15b might portray a borehole sample in the upper part of the partial annealing zone, with short track lengths and very few tracks at high angles to the *c*-axis. In each case, there is no apparent difference between angular or length distributions found with and without Cf irradiation—except for two isolated high-angle tracks in Fig. 15b, and the slightly higher $MTL_{Cf}$ values as noted before.

Use of $^{252}$Cf-derived fission fragments might be presumed to modify sampling of track lengths but exactly how it does so is unclear. The slight, but systematic trend to longer lengths in the Cf-irradiated samples, although not significant at two standard errors, may suggest a rather subtle bias. Simplistically, the introduction of additional etching conduits may increase the probability of intersecting longer tracks at the expense of shorter tracks, in effect a variation of the normal TINT length bias (Laslett et al., 1982). Each effect would explain why $MTL_{Cf}$ is longer. The broad similarity of etch pit size of a normal uranium fission track and a $^{252}$Cf track (in Fulford apatite $D_{par}$ for U-FT = 1.88 ± 0.02 μm and $D_{par}$ for $^{252}$Cf track = 2.20 ± 0.03 μm; $n = 50$ for each) argues that the Cf tracks are equivalent to semi-tracks. Since the length and angle results for samples with and without Cf irradiation are broadly similar, the differences only slightly exceeding the baseline measure of replicate analysis by one

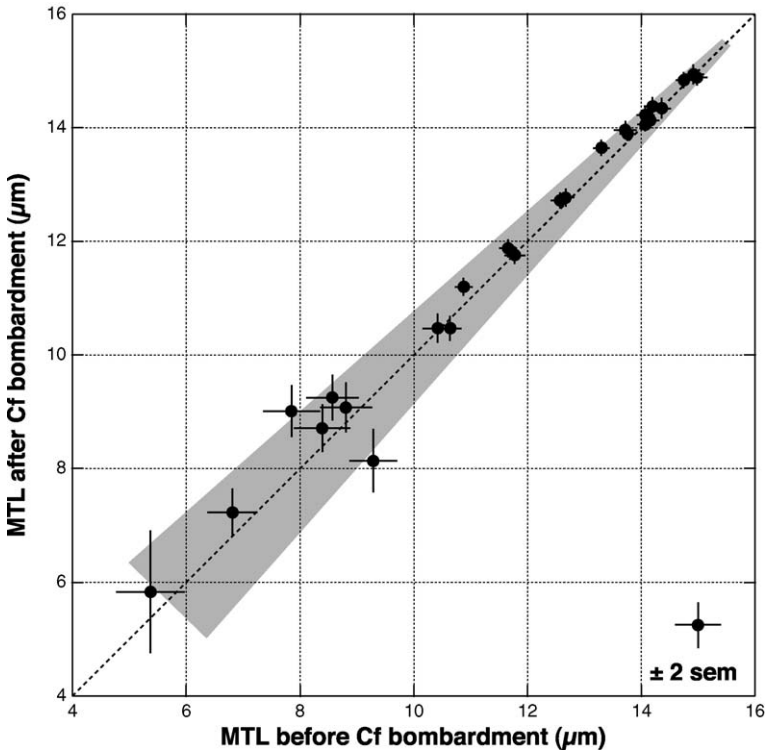


Fig. 14. Relationship between MTLs for the same apatite samples measured with and without $^{252}$Cf fission fragment irradiation by one analyst. The grey area corresponds to an estimate of $\pm 2$ standard errors found in replicate measurement by single analyst (see Fig. 3). Samples contained induced tracks, partially annealed in laboratory experiments and etched using 5 M $HNO_3$, $20 \pm 1$ °C, 20 s; TINTs only measured; ~ 100 tracks per measurement.

observer, this gives confidence in using $^{252}$Cf irradiation to reveal confined tracks and to enable robust analysis of certain samples which otherwise would have inadequate data.

## 7. Bias in measurement

Variation resulting from the measuring process can derive from three main sources: the observer (see Section 4), the equipment and procedures employed, and the size of the dataset.

### *7.1. Equipment and procedures*

Variations introduced from track-length measuring equipment and procedures are mainly systematic: with identical methodologies being applied to all analyses within one laboratory, differences should be chiefly interlaboratory.

The precision of the measuring system derives from a variety of factors, e.g.

- digitising tablets with different grid wire spacing and hence levels of resolution (or with unreported differing *X* and *Y* resolutions, producing disastrous consequences);
- the use of different calibration scales or stage micrometers;
- optical distortion in the drawing tube of the digitising tablet field of view;
- the size and location of the LED relative to the fission-track end.

Care in selecting and operating length measurement systems should maximise precision which may

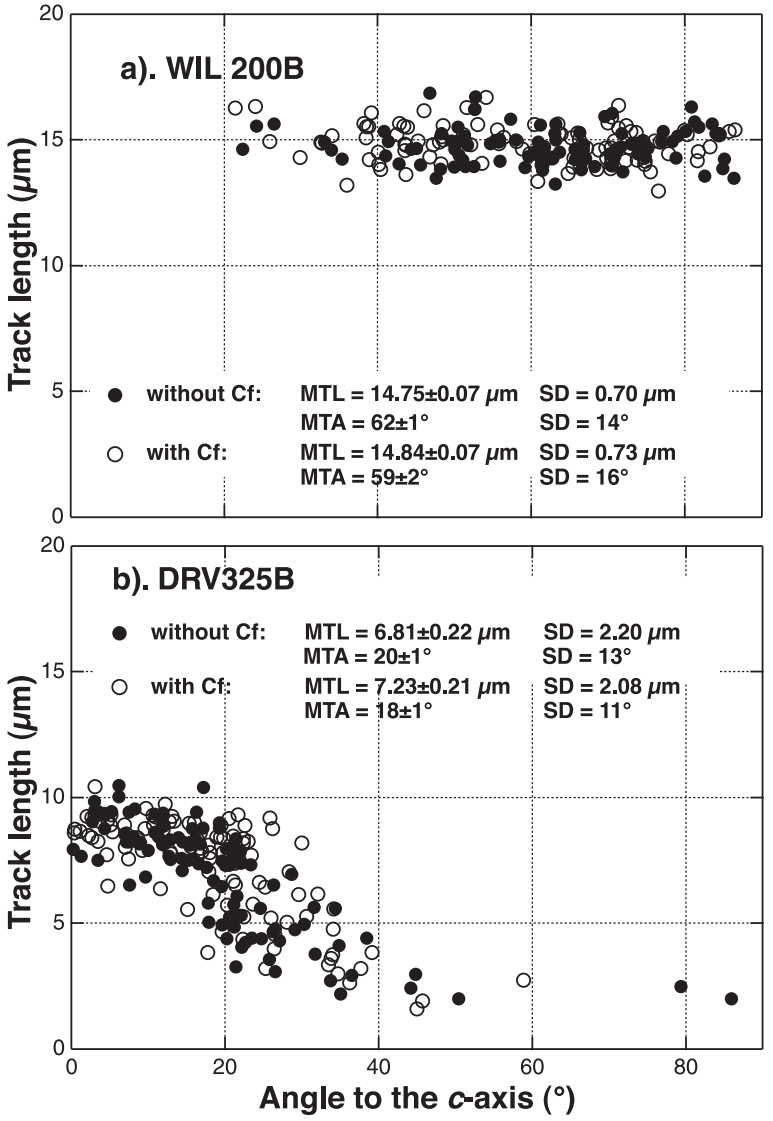


Fig. 15. Track length and angle distribution for two partially annealed apatite samples measured with and without $^{252}$Cf fission fragment irradiation. These samples represent two situations where Cf irradiation may be useful for FT studies; (a) young samples with long tracks, but low track densities, e.g. Himalayan type; (b) samples with very short tracks and low track density, e.g. borehole type. Samples etched 5 M $HNO_3$, 20 ± 1 °C, 20 s. TINTs only measured by a single analyst.

be tested in terms of the reproducibility: we assess the precision of our measuring systems to be better than 99% (see Section 2). However, we are not aware of any formal comparison of measuring systems between laboratories, and thus an implicit assumption of similarity of function and precision remains untested.

Differences in microscope configuration also result in variation, in particular the use of dry or oil immersion objective. Gleadow et al. (1986) concluded that the lack of contrast of confined tracks under oil makes them difficult to identify. From the results of an unpublished comparison of oil vs. dry objectives, we

would concur. Importantly, using oil, we found it more difficult to determine with confidence the ends of tracks and also to assess the orientation of the surface etch pits, essential to discriminate the *c*-axis parallel apatite sections with high etching efficiency.

### 7.2. Sample size

The size of a FT dataset defines the precision of an analysis: MTL, its standard deviation and the detailed track-length distribution are each dependent on the number of track lengths measured. Many analysts aim to measure 100 lengths. Rahn and Seward (2000) have suggested that, depending on the complexity of the distribution, no significant variation is found after 30 to 50 length measurements. We have examined the variation of results in several samples with MTL ranging between 8 and 10 μm, measuring 200 lengths in each and then plotting the data incrementally by groups of 10 lengths as measured. We found that the MTL stabilises depending on the sample between 50 and 120 tracks. Fig. 16 presents the evolution of MTL for one sample with a complex length pattern, the marked decrease from initial measurements perhaps resulting from familiarisation with the sample by the analyst and an enhanced perception of short tracks.

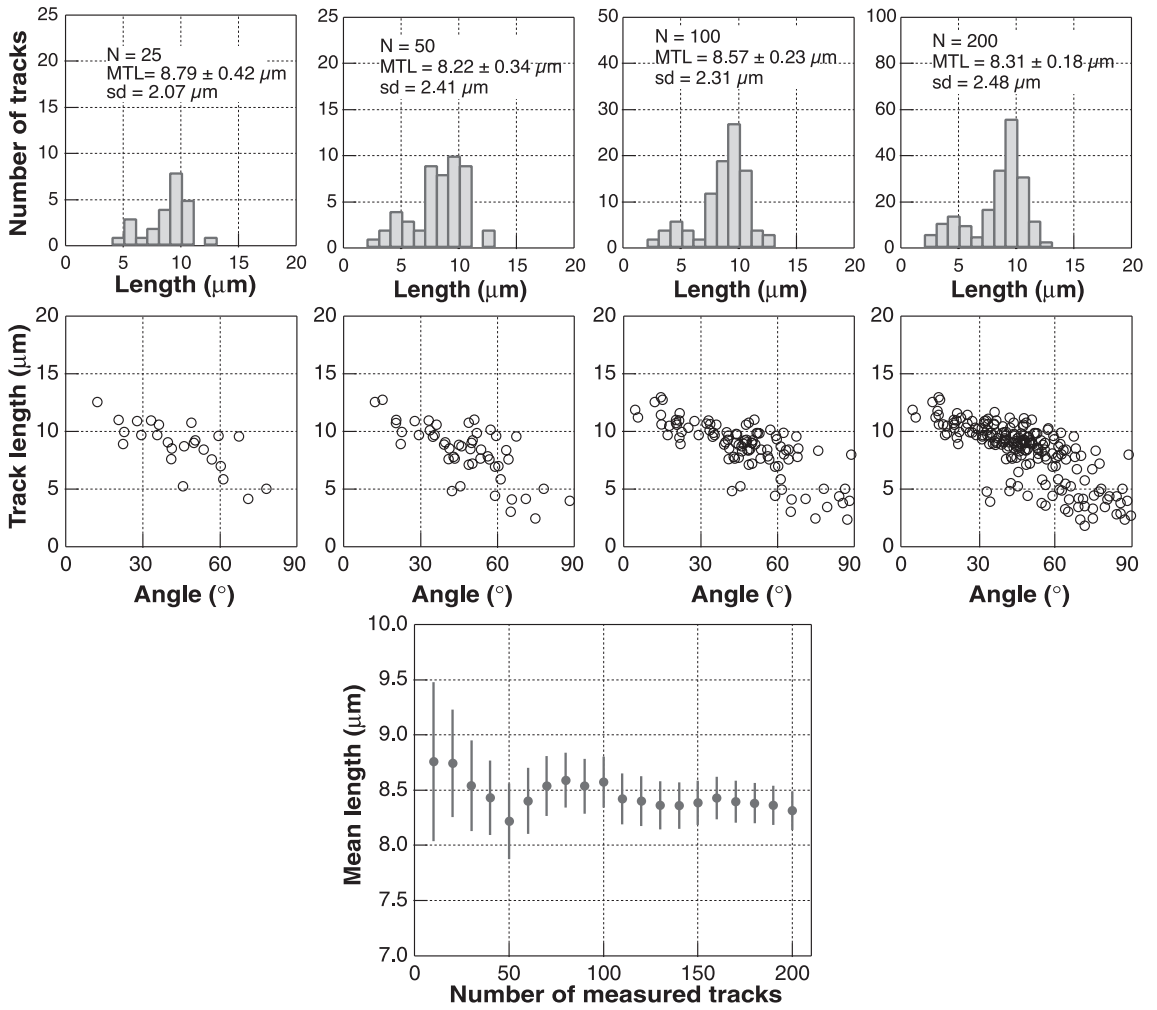


Fig. 16. Variation of track length and angle with the number of tracks measured for apatite sample MIN320B containing partially annealed, induced tracks. Etched 5 M $HNO_3$, 20 ± 1 °C 20 s; TINTs only; single analyst.

This sampling bias controls the value of the MTL and the shape of the track-length distributions. The proportion of short tracks, which are more difficult to determine, varies with the number of tracks measured. The greater the level of annealing, the larger the number of track lengths required to define a length distribution. This is purely a sampling problem. As annealing increases so does the number of short tracks. These are harder to observe and so more sampling is required. For a complex thermal history where there may be evidence within the track-length data for more than one event, it may be important to sample short tracks at all angles. One hundred track lengths may then represent the minimum needed to be representative of a population, and that below 100 lengths additional uncertainty may arise.

## 8. Track angle and short tracks

The observations presented above show that variation exists in track-length measurement which, in some cases, exceeds the frequently assumed uncertainty assessed from the standard error of the mean value. While methodology can introduce significant variation, observer bias also produces dispersion of data. Our results reinforce observations of previous workers that the angle of a track to the *c*-axis has a significant, probably major affect on the measured length. This affect is a summation of inter-related contributions from annealing and etching anisotropies together with observer bias: tracks are easier to see and measure at certain angles than at others because of their size and shape. This problem may be exacerbated at increased annealing levels where the track distribution is more complex and tracks at certain angles more difficult to see.

How to use track-angle data quantitatively is not immediately clear. Such data can provide a form of quality control for an analysis in which the measurement of track-length distribution alone cannot supply. Plotting track length vs. track angle can reveal anomalous data points, which may be attributed to poor technique or possibly a poor sample. Fig. 17 shows the results obtained by three analysts on measuring TINTs in a strongly annealed sample. The same clear trend of decreasing track length with increasing angle is apparent in each plot (cf. Fig. 7), but Analyst B alone reported a small number of anomalous longer tracks at high angles. Re-examination of this analysis suggests that these tracks were not TINTs but

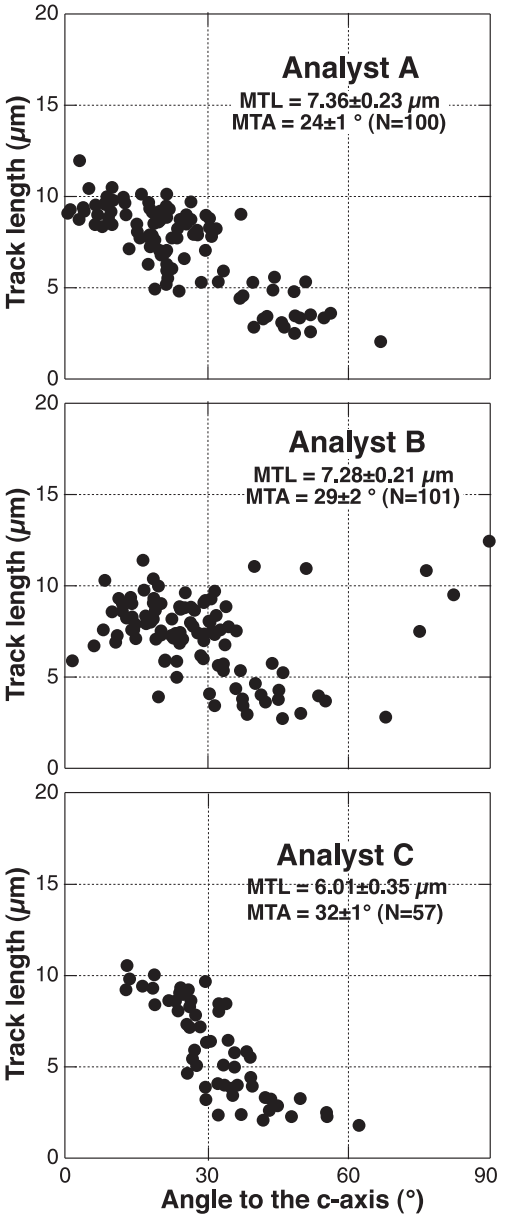


Fig. 17. Track length vs. angle to the *c*-axis relationship for the apatite sample DRV320B measured by three analysts. Etched 5 M $HNO_3$, 20 ± 1 °C, 20 s; TINTs only measured. The general trend is decreasing track length with increasing angle, except for analyst B; long tracks at high angles are anomalous and may be TINCLEs.

TINCLEs, with their concomitant observational bias (cf. Fig. 13c). Analyst B's results are thus biased, inappropriately, toward longer lengths, albeit in < 10% of the data in this case. Nevertheless, such a bias would transfer directly to thermal history modelling and its geological interpretation.

The enhanced angle sampling bias experienced when tracks are short may represent a major source of poor reproducibility between analysts (see Fig. 6). Short tracks have an angle to the *c*-axis ranging between 45° and 90°, the highest frequency being for the higher angles. This prompts the question whether measurement of short tracks (< 8 μm) has any specific value? The minimum measurable track length lies somewhere between 2 and 5 μm; depending on apatite composition, below 2 μm it is impossible to discriminate short confined tracks from etch pits.

The nature of short tracks has been questioned: are they fully etched? Green et al. (1986) proposed a gap model to explain the presence of short tracks. The presence of unetchable gaps in an annealed track inhibits the etching process, resulting in a fragmented track, each part of which may be identified as a short track. Fig. 18 shows in the same area long confined tracks oriented close to the *c*-axis, short tracks perpendicular to the *c*-axis and two tracks with the same alignment which could represent a gapped track. Hejl (1995) has argued that such unetchable gaps may occur in longer, even freshly induced tracks. TEM imaging of unetched tracks in apatite similarly shows that "gaps" exist (Paul and Fitzgerald, 1992). How frequently gapped tracks occur and what proportion of a population of short tracks is comprised of gapped tracks remain unresolved questions.

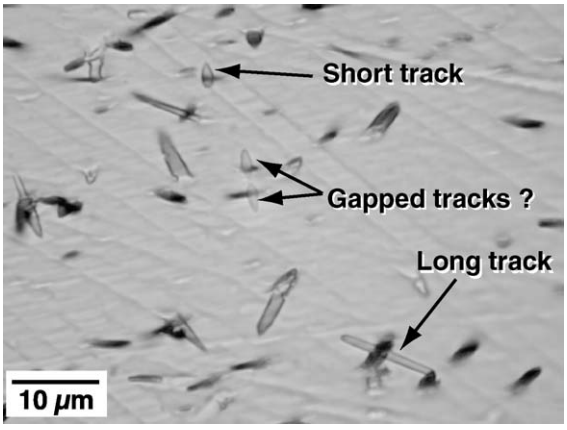


Fig. 18. Confined tracks observed in a partially annealed Durango apatite sample comparing long, short and possibly gapped tracks. Sample etched 5 M $HNO_3$, 20 ± 1 °C, 30 s. Transmitted illumination, dry objective.

Step-etch experiments between 20 and 60 s were carried out on two strongly annealed samples containing high track densities which increase the probability of intersection and revelation of TINTs. With increasing etching time, MTL increases slightly with the background bulk etch rate (Fig. 19), but short tracks (< 5 μm) are still present after 60 s of etching. With such prolonged etching, any unetched wall in a gapped track might be expected to have been removed (cf. Green et al., 1986). The similarity of distributions after different etch times suggests that if gapped tracks exist, they do not dominate and thus etching bias cannot explain all short tracks.

Clearly short tracks are problematic but they do indicate that a sample has been to high levels of annealing and thus they provide a qualitative thermal indicator. However, at such annealing levels, a very small change of temperature is required to produce a significant variation in track length and thus length offers a rather imprecise monitor of temperature. This appears true in both nature and laboratory experiment. Most laboratory annealing studies have excluded experiments to produce short MTLs, which means that high levels of annealing are poorly defined empirically. However, the imprecision associated with short track-length measurement suggests that such experiments would have made only a modest contribution to improving that understanding. Where short tracks have been measured, the angular data need to be considered, either to correct the measured lengths according to their angle, or to define the upper boundary of the envelope of measured track lengths at different angles, assuming that lengths shorter than this upper limit are less precise. Utilisation of short tracks in sample data and predictive modelling may be ambiguous. Some modelling procedures will predict short tracks but will bias them using their inherently greater uncertainty. However, the presence of a few short tracks in a sample dataset may have a significant affect on the modelling procedure. For zircon, Yamada et al. (1995) have suggested that length data should be modelled using only those tracks with

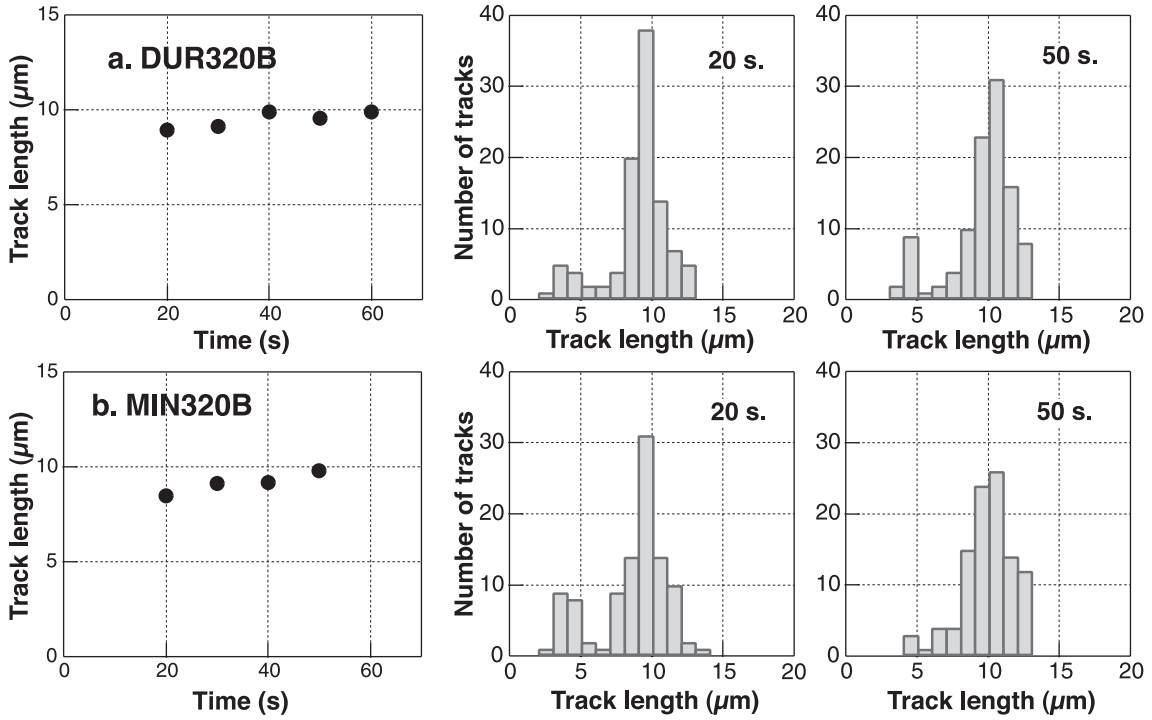


Fig. 19. Step-etch experiments for two strongly annealed apatite samples with track-length distributions shown for 20 and 50 s etching, 5 M $HNO_3$, 20 ± 1 °C. Short tracks are still present after prolonged etching. Single analyst; TINTs only; uncertainties within plotted points.

angles >60° to the *c*-axis to eliminate anisotropy in length distribution.

Clearly incorporating short tracks and angular data into the annealing algorithm is essential, but beyond the scope of this contribution, although we note that Ketcham et al. (1999) did indeed include angle in their annealing model.

We hope our observations and comments will stimulate further interest in the use of track angle data to refine thermal history prediction.

## 9. Conclusions

- Variation in confined fission-track length measurement in apatite frequently exceeds uncertainty assessed from the standard error. Replication of track-length measurement by an experienced single analyst gives uncertainties typically ~ 3%, which can rise to 18%. Inter-analyst variation using the same sample, methodology and equipment is typically ~ 5%, but in extreme cases can be ~ 30%. Uncertainty representative of differences between analysts might be better represented by quoting two standard errors. However, use of simple statistics as presented here may not be strictly valid if the measured parameters do not possess a Normal or Gaussian distribution—a more detailed treatment of these data is in progress.
- Sources of variation include differences in track revelation and biases in measurement and by observers.
- Comparison of two commonly used etchants reveals differences, with 0.8 M $HNO_3$ etching more isotropically but producing less well-defined tracks and failing to reveal *c*-axis parallel sections adequately where geometry is better understood. 5 M $HNO_3$ of is preferred as etchant.
- Different MTLs and distributions are found for TINTs and TINCLEs in the same sample for all but the longest lengths. For more heavily annealed samples with MTL values < 12 μm, TINCLEs are

substantially longer than TINTs with relatively few short TINCLEs at high angles. Measurement of TINCLEs effectively masks the anisotropy of annealing.

- Irradiation with $^{252}$Cf fission fragments is an effective way to increase the number of TINTs measured in a sample. Comparison of unirradiated and Cf-irradiated aliquots suggests an overall deviation of $\sim$ 3%, not exceeding that found for replicate analysis by a single analyst. Where MTL $< \sim$ 14 μm, a slight systematic shift to longer values for the Cf-irradiated samples is seen, possibly indicating the action of a subtle measurement bias.
- We suggest that 100 track lengths represent the minimum number representative of the track population.
- Track-length distributions are anisotropic and strongly controlled by track orientation, anisotropy increasing with annealing level. Track angle has a profound affect on measured length, summing together contributions from annealing and etching anisotropies as well as observer bias. Track angle should be accommodated within the annealing algorithm.
- The measurement of short tracks ($<5$ μm) is important as they strongly modify MTL and the length distribution, even though at high annealing levels, track length can change rapidly. Criteria used for the measurement of such tracks need to be standardised and defined before being used in annealing algorithms.
- We recommend that the same track revelation and observation conditions are used for the analysis of samples as are used in the empirical measurement of annealing and subsequently embodied in thermal history predictive models.

This study compares results between experienced analysts working with the same sample mounts, using the same equipment and a similar methodological approach within one laboratory. Larger differences might be expected from interlaboratory comparisons, as indicated by Miller et al. (1993). No track-length standards are available for interlaboratory comparison, other than freshly induced and volcanic-type distributions. Similarly, there is no formal comparison of measuring systems between laboratories, and thus an implicit assumption of similarity of function and precision remains untested. In the same way that age standards and the zeta calibration approach have provided rigour for FT age measurement, we propose that apatite FT length "standards" should be fabricated to facilitate interlaboratory comparison of track-length data and hence derive a more robust baseline for thermal history prediction.

## Acknowledgements

Some of the ideas embodied in this contribution have been considered previously by colleagues in either published form or in discussion. We have endeavoured to build on and quantitatively evaluate these ideas within a coherent consideration of track-length variation. Previous contributions by Ray Donelick and Paul Green especially must be acknowledged, and thanks are also due to them for constructive criticism. We thank Elf EP and Fred Walgenwitz for the generous financial support and encouragement during these studies. JB received a Marie Curie Fellowship from the European Community Programme Energy, Environment and Sustainable Development under Contract Number ENK6-CT-1999-50002. We are grateful to Ray Donelick for the assistance in setting up Cf irradiation. Rex Galbraith and other colleagues offered valuable comments on early thoughts and drafts of this paper, while Andy Gleadow and an anonymous referee made improvements to the first version. Especial thanks to Torgeir Garmo, Bill Kettley, Bart Kowallis, Rob Lavinsky, Gunnar Raade and Richard Tayler for their help in locating and supplying various apatite crystals. **[PD]**

## References

Barbarand, J., Pagel, M., 2001. Contrôle de la cicatrisation des traces de fission dans les cristaux d'apatite: le rôle de la composition chimique; importance of the chemistry to characterise apatite fission track annealing. C. R. Acad. Sci., Ser. IIa Earth Planet. Sci. 332, 259–265.

Barbarand, J., Carter, A., Wood, I.G., Hurford, A.J., 2003. Compositional and structural control of apatite fission-track annealing. Chem. Geol. 198, 107–137 (this issue).

Bhandari, N., Bhat, S.G., Rajagopalan, G., Tamhane, A.S., Venka-

tavaradan, V.S., 1971. Fission fragment tracks in apatite: recordable tracks lengths. Earth Planet. Sci. Lett. 13, 191–199.

Burtner, R.L., Nigrini, A., Donelick, R.A., 1994. Thermochronology of lower Cretaceous source rocks in the Idaho–Wyoming thrust belt. Am. Assoc. Pet. Geol. Bull. 78, 1613–1636.

Carlson, W.D., Donelick, R.A., Ketcham, R.A., 1999. Variability of apatite fission-track annealing kinetics: I. Experimental results. Am. Mineral. 84, 1213–1223.

Carter, A., 1999. Present status and future avenues of source region discrimination and characterization using fission track analysis. Sediment. Geol. 124, 31–45.

Crowley, K.D., Cameron, M., Schaefer, R.L., 1991. Experimental studies of annealing of etched fission tracks in fluorapatite. Geochim. Cosmochim. Acta 55, 1449–1465.

Donelick, R.A., 1991. Crystallographic orientation dependence of mean etchable fission track length in apatite: an empirical model and experimental observations. Am. Mineral. 76, 83–91.

Donelick, R.A., 1993. Apatite etching characteristics versus chemical composition. Nucl. Tracks Radiat. Meas. 21, 604.

Donelick, R.A., Miller, D.S., 1991. Enhanced TINT fission track densities in low spontaneous track density apatites using $^{252}$Cf-derived fission fragment tracks: a model and experimental observations. Nucl. Tracks Radiat. Meas. 18, 301–307.

Donelick, R.A., Roden, M.K., Mooers, J.D., Carpenter, B.S., Miller, D.S., 1990. Etchable length reduction of induced fission tracks in apatite at room temperature ( ~ 23 °C): crystallographic orientation effects and "initial" mean lengths. Nucl. Tracks Radiat. Meas. 17, 261–265.

Donelick, R.A., Ketcham, R.A., Carlson, W.D., 1999. Variability of apatite fission-track annealing kinetics: II. Crystallographic orientation effects. Am. Mineral. 84, 1224–1234.

Duddy, I.R., Green, P.F., Laslett, G.M., 1988. Thermal annealing of fission tracks in apatite 3: variable temperature behaviour. Chem. Geol. 73, 25–38.

Fitzgerald, P.G., Sorkhabi, R.B., Redfield, T.F., 1995. Uplift and denudation of the central Alaska range: a case study in the use of apatite fission track thermochronology to determine absolute uplift parameters. J. Geophys. Res. 100, 20175–20191.

Fleischer, R.L., Hart, H.R., 1972. Fission track dating: techniques and problems. In: Bishop, W.W., Miller, J.A., Cole, S. (Eds.), Calibration of Hominoid Evolution, vol. 135. Scottish Academic Press, Edinburgh, p. 170.

Galbraith, R.F., Laslett, G.M., 1996. Statistical modelling of thermal annealing of fission tracks in apatite. Geochim. Cosmochim. Acta 60, 5117–5131.

Galbraith, R.F., Laslett, G.M., Green, P.F., Duddy, I.R., 1990. Apatite fission track analysis: geological thermal history analysis based on a three-dimensional random process of linear radiation damage. Philos. Trans. R. Soc. Lond., A 332, 419–438.

Gallagher, K., 1995. Evolving temperature histories from apatite fission-track data. Earth Planet. Sci. Lett. 136, 421–435.

Gallagher, K., Hawkesworth, C.J., Mantovani, M.S.M., 1994. The denudation history of the onshore continental margin of SE Brazil inferred from apatite fission-track data. J. Geophys. Res. 99, 18117–18145.

Gallagher, K., Brown, R.W., Johnson, C.J., 1998. Geological applications of fission-track analysis. Annu. Rev. Earth Planet. Sci. 26, 519–572.

Gleadow, A.J.W., 1981. Fission-track dating methods: what are the real alternatives? Nucl. Tracks 5, 3–14.

Gleadow, A.J.W., Duddy, I.R., Green, P.F., Lovering, J.F., 1986. Confined fission track lengths in apatite: a diagnostic tool for thermal history analysis. Contrib. Mineral. Petrol. 94, 405–415.

Green, P.F., 1981. "Track-in track" length measurements in annealed apatites. Nucl. Tracks 5, 121–128.

Green, P.F., 1988. The relationship between track shortening and fission track age reduction in apatite: combined influences of inherent instability, annealing anisotropy, length bias and system calibration. Earth Planet. Sci. Lett. 89, 335–352.

Green, P.F., 1995. AFTA Today. On Track (unpublished Newsletter of the International Fission-Track Community) 5, 8–10.

Green, P.F., Durrani, S.A., 1977. Annealing studies of tracks in crystals. Nucl. Tracks 1, 33–39.

Green, P.F., Duddy, I.R., Gleadow, A.J.W., Tingate, P.R., Laslett, G.M., 1986. Thermal annealing of fission tracks in apatite: 1. A qualitative description. Chem. Geol., Isot. Geosci. Sect. 59, 237–253.

Green, P.F., Duddy, I.R., Gleadow, A.J.W., Lovering, J.F., 1989a. Apatite fission-track analysis as a paleotemperature indicator for hydrocarbon exploration. In: Naeser, N.D., Mc Culloh, Th.H. (Eds.), Thermal History of Sedimentary Basins. Springer Verlag, New York, pp. 181–195.

Green, P.F., Duddy, I.R., Laslett, G.M., Hegarty, K.A., Gleadow, A.J.W., Lovering, J.F., 1989b. Thermal annealing of fission tracks in apatite 4: quantitative modelling techniques and extension to geological timescales. Chem. Geol. 79, 155–182.

Hegarty, K., 2000. FT2000—Congratulations to the organizers and comments on the way forward. On Track (unpublished Newsletter of the International Fission-Track Community) 10, 17–20.

Hejl, E., 1995. Evidence for unetchable gaps in apatite fission tracks. Chem. Geol., Isot. Geosci. Sect. 122, 259–269.

Hurford, A.J., 1990. Standardization of fission track dating calibration: recommendation by the Fission Track Working Group of the I.U.G.S. Subcommission on Geochronology. Chem. Geol., Isot. Geosci. Sect. 80, 171–178.

Hurford, A.J., Green, P.F., 1983. The Zeta age calibration of fission-track dating. Chem. Geol., Isot. Geosci. Sect. 1, 285–317.

Jonckheere, R., Wagner, G.A., 2000. On the occurrence of anomalous fission tracks in apatite and titanite. Am. Mineral. 85, 1744–1753.

Ketcham, R.A., 2000. Some thoughts on inverse modelling and length and kinetic calibration. On Track (unpublished Newsletter of the International Fission-Track Community) 10, 8–14.

Ketcham, R.A., Donelick, R.A., Carlson, W.D., 1999. Variability of apatite fission-track annealing kinetics: III. Extrapolation to geological time scales. Am. Mineral. 84, 1235–1255.

Lal, D., Rajan, R.S., Tamhane, A.S., 1969. Chemical composition of nuclei of Z>22 in cosmic ray using meteoritic minerals as detectors. Nature 221, 33–37.

Laslett, G.M., Kendall, W.S., Gleadow, A.J.W., Duddy, I.R., 1982.

Bias in measurement of fission-track length distributions. Nucl. Tracks 6, 79–85.

Laslett, G.M., Gleadow, A.J.W., Duddy, I.R., 1984. The relationship between fission-track length and track density in apatite. Nucl. Tracks 9, 29–38.

Laslett, G.M., Green, P.F., Duddy, I.R., Gleadow, A.J.W., 1987. Thermal annealing of fission tracks in apatite: 2. A quantitative analysis. Chem. Geol., Isot. Geosci. Sect. 65, 1–13.

Lutz, T.M., Omar, G., 1991. An inverse method of modeling thermal histories from apatite fission-track data. Earth Planet. Sci. Lett. 104, 181–195.

Miller, D.S., Crowley, K.D., Dokka, R.K., Galbraith, R.F., Kowallis, B.J., Naeser, C.W., 1993. Results of interlaboratory comparison of fission-track ages for the 1992 fission track workshop. Nucl. Tracks Radiat. Meas. 21, 613.

Paul, T.A., Fitzgerald, P.G., 1992. Transmission electron microscopic investigation of fission tracks in fluorapatite. Am. Mineral. 77, 336–344.

Rahn, M., Seward, D., 2000. How many track lengths do we need? On Track (unpublished Newsletter of the International Fission-Track Community) 10, 14–17.

Singh, S., Singh, D., Sandhu, A.S., Singh, G., Virk, H.S., 1986. A study of track etch anisotropy in apatite. Nucl. Tracks 12 (1–6), 927–930.

Watt, S., Durrani, S.A., 1985. Thermal stability of fission tracks in apatite and sphene: using confined track length measurements. Nucl. Tracks 10, 349–357.

Willett, S.D., 1997. Inverse modeling of anealing of fission tracks in apatite 1: a controlled random search method. Am. J. Sci. 297, 939–969.

Yamada, R., Tagami, T., Nishimura, S., Ito, H., 1995. Annealing kinetics of fission tracks in zircon: an experimental study. Chem. Geol., Isot. Geosci. Sect. 122, 249–258.

Yamada, R., Yoshioka, T., Watanabe, K., Tagami, T., Nakamura, H., Hashimoto, T., Nishimura, S., 1998. Comparison of experimental techniques to increase the number of measurable confined fission tracks in zircon. Chem. Geol. 149, 99–107.